Published in final edited form as:

Biochim Biophys Acta. 2017 June ; 1858(6): 442–458. doi:10.1016/j.bbabio.2017.03.005.

Identity and function of a cardiac mitochondrial small conductance Ca^{2+}-activated K^+ channel splice variant

MeiYing Yang[a], **Amadou K.S. Camara**[a,e], **Mohammed Aldakkak**[a,1], **Wai-Meng Kwok**[a,c,e], and **David F. Stowe**[a,b,d,e,f,*]

[a]Department of Anesthesiology, Medical College of Wisconsin, Milwaukee, WI, USA

[b]Department of Physiology, Medical College of Wisconsin, Milwaukee, WI, USA

[c]Department of Pharmacology and Toxicology, Medical College of Wisconsin, Milwaukee, WI, USA

[d]Department of Biomedical Engineering, Medical College of Wisconsin and Marquette University, Milwaukee, WI, USA

[e]Cardiovascular Center, Medical College of Wisconsin, Milwaukee, WI, USA

[f]Research Service, Zablocki VA Medical Center, Milwaukee, WI, USA

Abstract

We provide evidence for location and function of a small conductance, Ca^{2+}-activated K^+ (SK_{Ca}) channel isoform 3 (SK3) in mitochondria (m) of guinea pig, rat and human ventricular myocytes. SK_{Ca} agonists protected isolated hearts and mitochondria against ischemia/reperfusion (IR) injury; SK_{Ca} antagonists worsened IR injury. Intravenous infusion of a SK_{Ca} channel agonist/antagonist, respectively, in intact rats was effective in reducing/enhancing regional infarct size induced by coronary artery occlusion. Localization of SK3 in mitochondria was evidenced by Western blot of inner mitochondrial membrane, immunocytochemical staining of cardiomyocytes, and immunogold labeling of isolated mitochondria. We identified a SK3 splice variant in guinea pig (SK3.1, aka SK3a) and human ventricular cells (SK3.2) by amplifying mRNA, and show mitochondrial expression in mouse atrial tumor cells (HL-1) by transfection with full length and truncated SK3.1 protein. We found that the Nterminus is not required for mitochondrial trafficking but the C-terminus beyond the Ca^{2+} calmodulin binding domain is required for Ca^{2+} sensing to induce mK^+ influx and/or promote mitochondrial localization. In isolated guinea pig mitochondria and in SK3 overexpressed HL-1 cells, mK^+ influx was driven by adding $CaCl_2$. Moreover, there was a greater fall in membrane potential ($\Delta\Psi_m$), and enhanced cell death with simulated cell

*Corresponding author at: Department of Anesthesiology Research Division, Medical College of Wisconsin, M4280, 8701 Watertown Plank Road, Milwaukee, WI 53226, USA. dfstowe@mcw.edu (D.F. Stowe).

[1]Present address: Department of Surgical Oncology, Medical College of Wisconsin, Milwaukee, WI, USA.

Appendix A. Supplementary methods and results

Supplementary data to this article can be found online at http://dx.doi.org/10.1016/j.bbabio.2017.03.005.

Disclosures

Conflict of interest

The authors have nothing to disclose concerning any conflict of interest.

Transparency document

The http://dx.doi.org/10.1016/j.bbabio.2017.03.005 associated with this article can be found, in online version.

injury after silencing SK3.1 with siRNA. Although SK_{Ca} channel opening protects the heart and mitochondria against IR injury, the mechanism for favorable bioenergetics effects resulting from SK_{Ca} channel opening remains unclear. SK_{Ca} channels could play an essential role in restraining cardiac mitochondria from inducing oxidative stress-induced injury resulting from mCa^{2+} overload.

Keywords

Cardiac mitochondria; Inner mitochondrial membrane; Cell signaling; Ischemia reperfusion injury; Oxidant stress; Small conductance Ca^{2+}-sensitive K^+ channel

1. Introduction

Small conductance Ca^{2+}-activated K^+ channels may perform many roles including protection against cardiac ischemia and reperfusion (IR) injury and therefore warrant additional studies regarding their location and function, particularly in mitochondria. From this knowledge novel, targeted therapeutic strategies may be developed to reduce IR injury. K_{Ca} channels of intermediate or small conductances are calmodulin (CaM)-dependent, and gated primarily by Ca^{2+} [1-4]. These channels have small unit conductances of 3–30 (small, SK_{Ca}) and 20–90 (intermediate IK_{Ca}) pS [5]. The opening of SK_{Ca} channels is initiated by Ca^{2+} binding to calmodulin within the C-terminus of the channel that then forms a dimer [6,7]. SK_{Ca} channels are widely expressed in different cells [8] including blood, nerve, endothelial, and smooth, skeletal and cardiac myocytes. There are at least three known genes encoding SK_{Ca} channels. The $K_{Ca}2.3$ (aka SK3) isoform was identified first in endothelial cells and found to exert a potent, tonic hyperpolarization that reduced vascular smooth muscle tone [9]. A decrease in endothelial IK_{Ca} and SK_{Ca} currents and decreased endothelial cell IK_{Ca} expression during hypoxia and reoxygenation (HR) was associated with a decrease in EDHF-mediated relaxation of porcine coronary arteries [10]. In contrast, activation of IK_{Ca}/SK_{Ca} channels with 1-EBIO enhanced the K^+ current that was blunted by HR and restored EDHF-mediated relaxation [10]. These data indicated that IK_{Ca}/SK_{Ca} channels are important for protecting the endothelium against HR injury. The $K_{Ca}2.2$ (SK2) isoform was first found in mouse and human heart cell membranes using Western blot analysis and reverse transcription polymerase chain reaction (RT-PCR) [11]. Later, Tuteja et al. [12] quantified SK1, SK2, and SK3 transcripts between atria and ventricles from single, isolated mouse cardiomyocytes and reported much greater expression of SK1 and SK2 in atria compared to ventricles, whereas SK3 levels were similar in both tissues. There was also much greater atrial than ventricular sensitivity to action potential (AP) repolarization by apamin [12], a selective SK_{Ca} antagonist [11,13].

The cardioprotective roles of SK_{Ca} [14], IK_{Ca}, [10], and BK_{Ca} (big) [15,16] channels in IR and HR injury have been reported previously by our lab and others. We tested the functionality of SK_{Ca} channel opening [14] by perfusing isolated hearts transiently before ischemia with the IK_{Ca} [1,4,17] and SK2 and SK3 [18-21] channel opener DCEBIO (DCEB). We found [14] that DCEB elicited pharmacologic pre-conditioning (PPC) protection in a manner similar to that of the BK_{Ca} channel opener NS1619 [16]; both the

specific SK_{Ca} antagonist NS8593 [22,23] and the ROS scavenger MnTBAP (TBAP), a dismutator of superoxide anion ($O_2^{\cdot -}$), abolished the cardioprotection [14]. Because excess reactive oxygen species (ROS) generation, depressed mitochondrial bioenergetics, and mCa^{2+} overload, are major factors underlying IR injury [24], this suggested SK_{Ca} channels may play a role in mitochondrial function. Indeed, Xu et al. [15] first identified the presence of BK_{Ca} channels in cardiac mitochondria.

Recently, Dolga et al. [25] found that the SK2 isoform was expressed in mitochondria of neuronal HT-22 cells. At about the same time, we furnished novel evidence for the presence of SK2 and SK3 isoforms in the inner mitochondrial membrane (IMM) of guinea pig isolated ventricular mitochondria [14]. Based on multiple evidence including mass spectroscopy analysis and immuno-gold electron microscopy, we found that SK_{Ca} channels are located in ventricular mitochondria, most likely within the IMM [14]. Functionally, we found that the SK_{Ca} channel opener DCEB, when given briefly before cardiac ischemia, reduced mitochondrial injury by reducing mitochondrial $[Ca^{2+}]$ overload and excess $O_2^{\cdot -}$ emission, and by improving the redox state during reperfusion [14].

In the present report we have extended our prior work [14] to further characterize the mSK_{Ca} channel, including its cardioprotective mechanism, and to identify the SK3 gene products in guinea pig, rat, and human heart. Our aims were: a) to localize and identify SK3 isoforms in guinea pig and human cardiac mitochondria; b) to identify the SK3 mitochondrial splice variant(s); c) to determine if the SK3 Cterminus downstream of the calmodulin binding domain is required for mitochondrial targeting; d) to furnish evidence that the Ca^{2+} sensor of SK3 faces the matrix; e) to determine if increased Ca^{2+} triggers K^+ uptake into mitochondria in HL-1 cells overexpressing SK3.1; f) to assess for cytoprotection against HR injury in HL-1 cells overexpressing SK3.1; and g) to examine for exacerbation of HR injury in SK3.1 silenced HL-1 cells.

2. Materials and methods

2.1. Isolated guinea pig heart global ischemia model

The investigation conformed to the *Guide for the Care and Use of Laboratory Animals* (NIH Publication 85-23, revised 1996). The appropriate committees at the Medical College of Wisconsin approved the use of guinea pig, rat, and human heart tissue prior to initiating this study. Guinea pig hearts (250–300 g) were isolated and prepared as described in detail [14,16,26-30]. Briefly, guinea pigs were anesthetized with ketamine (50 mg/kg) and treated with 1000 units of heparin; after thoracotomy, the hearts were immediately perfused via the aorta with cold Krebs-Ringer's perfusate. Hearts were instrumented with a saline-filled balloon attached to a transducer to measure isovolumetric LVP and the entire coronary vascular system was perfused via the aorta (retrograde flow) at constant pressure with Krebs-Ringer's solution at 37 °C. At 120 min reperfusion, hearts not isolated for their mitochondria were stained with TTC and infarct size was determined as a percentage of total ventricular heart weight [14,16,27,30].

Isolated guinea pig hearts (n =6 per drug group) were perfused with no drugs (control), test drugs (an SK_{Ca} agonist and or antagonist), or the ROS scavenger TBAP, alone or in

combination before and after 35 min global (no aortic or coronary flow) ischemia. The agonist or antagonist was given 15 min before ischemia and for 15 min during reperfusion. Developed left ventricular (LV) pressure, coronary flow and heart rate were recorded online before, during and after ischemia. Drugs given were: 3 μM DCEB, an opener of SK2, SK3 and IK_{Ca} channels [1,18-21]; 10μM NS8593, a specific antagonist of SK_{Ca} channels [22,23]; and 5 μM TBAP, a chemical dismutator of $O_2{\cdot}^-$ that can enter the mitochondrial matrix [31].

2.2. In vivo rat heart regional ischemia model

Adult rats (250–300 g, n =5 rats per drug group) of either sex were anesthestized, intubated, and artificial respiration was initiated. The right carotid artery was cannulated to monitor blood pressure continuously. After thoracotomy a suture was placed around the proximal LAD for reversible coronary artery occlusion that was verified by regional epicardial cyanosis. Hearts were subjected to 35 min LAD occlusion followed by 120 min reperfusion. For sham controls the LAD suture was placed but not tightened. Infarct size was assessed 120 min after the regional ischemia using the Evan's Blue area at risk and TTC staining techniques for viable tissue, and expressed as % area-at-risk. Drugs infused via the left jugular vein were saline (control), DCEB (30 μg/kg/min), or NS8593 (100 μg/kg/min) dissolved in physiological saline. Drugs were infused 15 min before and after LAD occlusion. Drug infusion in the shams had no effect on blood pressure. Infarct size measurements were blinded to the drug. We conducted the *in vivo* procedure in the rat because it is technically easier than in the guinea pig.

2.3. Ca^{2+}-induced K^+ uptake in isolated ventricular mitochondria

Matrix K^+ (mK^+) was measured as we reported previously [32]. Briefly, mitochondria were incubated with 1 μM PBFI-AM, a K^+ fluorescence dye (Invitrogen), in the isolation buffer (described in Supplemental materials, S.1) for 20 min at room temperature. The suspension was diluted with isolation buffer and then centrifuged twice to wash out extra-matrix residual dye. After entering the matrix, PBFI, in the acetylated methyl-ester (AM) form, is cleaved from the methylester by esterases and retained. The mitochondria pellet was resuspended to 0.5 mg protein/ml in a respiration buffer (described in Supplemental materials, S.2) containing (in mM) 130 KCl, 5 K_2HPO_4, 20 MOPS, 2.5 EGTA, and 0.1% BSA, and adjusted to pH 7.15 with KOH. The buffer also contained 200 μM ATP, 20 μM paxilline, and 100 nM TRAM-34, to prevent potential mK_{ATP}, BK_{Ca}, and IK_{Ca} channel opening, respectively. Mitochondria were energized with 10 mM pyruvate. Most experiments were conducted in the presence of 500 μM quinine to block mitochondrial K^+/H^+ exchange (mKHE) in order to prevent extrusion of K^+ that enters the matrix. To restrict mitochondrial Ca^{2+}-induced K^+ channel opening before beginning the experiments, the respiration buffer contained 2.5 mM EGTA, which chelates most of the Ca^{2+} in the buffer, so that [Ca^{2+}] was undetectable. After adding 0.2–3 mM $CaCl_2$ (in buffer with 2.5 mM EGTA), buffer and matrix [Ca^{2+}] can increase only within the nM range. This is apparent from a previous report [33] in which we measured external and matrix [Ca^{2+}] using a similar respiration buffer but containing 0.6 mM $CaCl_2$ and 1 mM EGTA; this resulted in an external [Ca^{2+}] of 300 nM and a matrix [Ca^{2+}] of 1000 nM. In buffer containing approximately 40 μM EGTA carried over with the mitochondria from the isolation buffer, with no added $CaCl_2$, we observed a basal external [Ca^{2+}] of 80–100 nM and a matrix

[Ca^{2+}] of 210–250 nM [34,35]. Mitochondrial K^+ was monitored in a cuvettebased spectrophotometer (QM-8, Photon Technology International, PTI) with excitation and emission light, λ_{ex} 340 and 380 nm; λ_{em} 500 nm, while adding 0–3 mM $CaCl_2$ to the buffer. In some experiments 10 nM valinomycin, a K^+ ionophore, was given to verify an increase in mK^+ influx and for referencing the change of K^+ influx induced by Ca^{2+} with or without UCL1684, another blocker of SK_{Ca} channels [36]. In other experiments cyclosporine A (CSA) or ruthenium 360 (Ru360) was given to prevent mPTP opening or to block Ca^{2+} uptake by the mitochondrial Ca^{2+} uniporter (MCU), respectively.

2.4. Isolation of rat/guinea pig ventricular cardiomyocytes and immunostaining of SK3 channels in rat cardiomyocytes

Cardiomyocytes were isolated from guinea pig and rat hearts by retrograde perfusion of isolated hearts with a collagenase containing solution as we reported previously [37,38]. First, hearts were removed from anesthetized rats or guinea pigs; the aorta was cannulated to perfuse the coronary circulation with solution A containing (in g/L): 11 MEME (Sigma), 1 glucose, and 2 $NaHCO_3$ at pH 7.23 for 5 min to clear blood. After blood was cleared, hearts were perfused for 20 min with a digestion solution containing 0.1% BSA, 75 U/ml collagenase Type II, and 1 unit/ml protease type XIV in solution A, at pH 7.23. Hearts were then removed from the perfusion apparatus and the ventricles were minced into small pieces in the digestion solution and incubated at 37 °C for 10 min in a shaker water bath to disperse the cells. Next the cell suspension was filtered and centrifuged at 300 rpm for 1 min and resuspended in 5 ml Tyrode buffer (in mM): 132 NaCl, 10 HEPES, 5 glucose, 5 KCl, 1 $MgCl_2$ without added $CaCl_2$, after which an equal volume of Tyrode buffer containing 1 mM $CaCl_2$ was slowly added. Freshly isolated guinea pig cardiomyocytes were used for amplification of SK_{Ca} channel variants.

Freshly isolated adult rat cardiomyocytes were plated in a Laminin coated Lab-Tek chamber and incubated at 37 °C for 2 h; next, myocytes were fixed with 4% paraformaldehyde in PBS for 15 min at room temperature followed by fixation for 5 min in ice cold (−20 °C) methanol. After washing three times with PBST (PBS+ 0.1% tween 20), myocytes were blocked and permeabilized with 20% goat serum with 1% BSA and 0.5% Triton X-100 in PBST for 1 h at room temperature. After washing, cardiomyocytes were incubated overnight at 4 °C with a combination of primary antibodies: goat anti-COX 1 (1:50 dilutions) and rabbit anti-SK3 (1:50 dilutions) diluted with 1% BSA and 0.2% Triton X-100 in PBST. The next day, myocytes were incubated with secondary antibodies, donkey anti-goat antibody conjugated to Alexa 546 and goat anti-rabbit antibody conjugated to Alexa FITC for 2 h at room temperature in the dark. Following another washing with PBST, myocytes were mounted on slides using SHUR/Mount™ Liquid Mounting Medium, TBS (VWR) and imaged with an A1R confocal microscope. Images were captured on 1024 × 1024 pixel CCDs with an oil immersion ×60 objective and were saved and visualized with NIS elements AR software. To quantitate the co-localization of SK3 with COX 1, solely a mitochondria protein, line scan analysis was performed with ImageJ to indicate the degree of overlap between the two signals. A line across the cardiomyocyte was drawn in the merged figure and the intensity profiles of all pixels of the two signals were plotted with a RGB profile plot program.

2.5. Amplification of SK_{Ca} channel variants from guinea pig ventricular myocytes and human ventricles

We first amplified SK_{Ca} from total RNA to determine if a gene encoding SK_{Ca} channels exists in human ventricles as well as in guinea pig ventricular myocytes. Total RNA was extracted from freshly isolated guinea pig cardiomyocytes or human ventricular tissue using RNeasy mini kit (Qiagen, Crawley, UK). cDNA was synthesized from 1 μg of total RNA with M-MLV reverse transcriptase and oligo(dT) primers and then subjected to PCR amplification using iproof HF master mix (Bio-Rad). The presence of SK1, SK2 and SK3 isoforms in guinea pig ventricular myocytes was detected using PCR primers (Table 1), which were designed based on coding sequence from GenBank sequence XM_ 003465180 for SK1, XM_003473180 for SK2 and XM_003475583 for SK3. The presence of the SK3 isoform in human ventricular tissue was detected using the following PCR primers: HSK3.1F1: 5′ -ATGGACACTTCTGGGCACTT- 3′ (forward) and HSK3.1R15′ -TCACGAAGAGCT-GGACTT- 3′ (reverse) for the amino acid (a.a.) 1–346; HSK3.1F2: 5′ –GATGTTTG GAATTGTTGTTATG-GTG- 3′ (forward) and HSK3.1R2 5′ -TTAGCAACTGCTTGAACTTGT-3′ (reverse) for a.a. 290–731. All human SK3 amplification primers were designed based on NM_001204087 coding sequence from GenBank. Reverse transcription-negative controls (no RT) were used to ensure that there was no genomic contamination in the RNA samples in each experiment. PCR products were analyzed by agarose gel electrophoresis and positive PCR products were sequenced.

2.6. HL-1 cell culture, plasmid construction and cell transfection

HL-1 cells, which are derived from a mouse atrial cardiomyocyte tumor lineage, were plated in tissue culture flasks coated with gelatin/fibronectin and maintained in claycomb medium supplemented with 10% FBS, 0.1 mM norepinephrine, 2 mM L-glutamine, 100 U/ml penicillin, and 100 μg/ml streptomycin. All cells were cultured at 37 °C with 5% CO_2 in a humidified incubator.

The full-length of SK3.1 ($SK3_{FL}$) was amplified from cDNA of guinea pig ventricular myocytes using SK3CF1: 5′-ACCTGCAGATGGACACTTCT-3′ as forward, and SK3CR1: 5′-ACGGATCCGCAACTGCTTGAACTTGT-3′ as reverse primer, and then inserted into the *Bam*HI and *Pst*I sites of the pEGFP-N3 vector in frame with the enhanced green fluorescence protein (EGFP) to construct $SK3_{FL}$-EGFP. The 1–277 a.a. truncated of SK3.1 ($SK3_{\Delta 1–277}$) ($_{\Delta}$=truncated a.a. sequence) was amplified from $SK3_{FL}$-EGFP plasmids using SK3CF3: 5′-ACCTGCAGATGCTGATTTTTGGGATGTTT-3′ as forward and SK3CR1 as reverse primers. The 626–720 a.a. truncated SK3.1 ($SK3_{\Delta 626–720}$) was also amplified from $SK3_{FL}$-EGFP plasmids using SK3CF1 as forward and SK3CR4: 5′-TCGGATCCGACGTTCTGCATCTTGGA-3′ as reverse primers. The $SK3_{\Delta 1–277}$ and $SK3_{\Delta 626–720}$ were also cloned into pEGFP-N3 vector individually through the *Bam*HI and *Pst*I sites to make $SK3_{\Delta 1–277}$–EGFP and $SK3_{\Delta 626–720}$–EGFP plasmids. All of the above constructs were verified by sequencing. HL-1 cells were transfected with plasmids $SK3_{FL}$-EGFP, $SK3_{\Delta 1–277}$–EGFP and $SK3_{\Delta 626–720}$–EGFP individually using jetPRIME Polyplus (New York) according to the manufacturer's protocol.

2.7. Mitochondrial localization of overexpressed SK3.1 in HL-1 cells

Localization of overexpressed SK3.1 in HL-1 cells was observed fluoroscopically using a laser scanning confocal microscope (Nikon AIR). HL-1 cells were plated on gelatin/fibronectin coated 35 mm glass bottom dishes (Matek, Ashland, MA) and were transfected individually with $SK3_{FL}$-EGFP, $SK3_{\Delta 1–277}$–EGFP and $SK3_{\Delta 626–720}$–EGFP. Forty-eight hours after cell transfection, the culture medium was replaced with Tyrode buffer and cells were loaded with a mitochondrial specific marker, Mitotracker red (MTR, 100 nM) for 30 min at 37 °C and then washed with Tyrode buffer. EGFP fluorescence was measured at λ_{ex}488 nm and at λ_{em} 515 nm; MTR was measured at λ_{ex}581 nm and at λ_{em}644 nm. Both EGFP and MTR were measured simultaneously. Mitochondrial localization was determined by colocalization of EGFPtagged SK3.1 full-length and truncated proteins with MTR. To quantitate the co-localization of SK3 with the mitochondrial marker MTR in transfected HL-1 cells, line scan analysis was performed with ImageJ as described in Section 2.4. Two lines around overexpressed $SK3_{FL}$ and truncated proteins were drawn in corresponding transfected cells and the intensity profiles for each line were analyzed separately using the ImageJ RGB profile plot program.

2.8. Determination of matrix K^+ uptake in SK3.1 overexpressed HL-1 cells

Matrix K^+ (mK^+) was measured in HL-1 cells using the K^+-sensitive fluorescent indicator PBFI; PBFI was loaded to favor mitochondrial localization as described previously [39]. HL-1 cells were grown on glass coverslips and individually transfected with $SK3_{FL}$-EGFP, $SK3_{\Delta 1–277}$–EGFP and $SK3_{\Delta 626–720}$–EGFP. After 48 h, cells were loaded with 10 μM PBFI AM for 60 min at 37 °C and then washed to remove residual extracellular PBFI. Coverslips were then mounted in a recording chamber onto the stage of an inverted microscope (Nikon Diaphot 200) with attached camera (CoolSNAPfx Photometrics) and perfused with a K^+-free mitochondrial buffer containing (in mM): 250 sucrose, 25 Tris, 3 EGTA, 5 $MgCl_2$, 5 Na-succinate and 5 glutamate (pH 7.3). PBFI fluorescence was recorded at emission λ_{em} 510 nm after sequential excitations at λ_{ex}340 nm and λ_{ex}380 nm (DG-4, Sutter, Novato, CA) and the λ340/380 nm ratio was determined using MetaFluor software (Universal Imaging Corporation, PA). After recording basal K^+ influx for 2–3 min, cells were permeabilized with 20 μM digitonin for 2 min, followed by perfusion with the K^+-free mitochondrial buffer. K^+ uptake activated by Ca^{2+} was determined by rapidly elevating bath concentrations of both K^+ and Ca^{2+}. To verify that a change in the PBFI λ340/380 nm ratio was due to matrix K^+ influx, 5 μM alamethicin, a 20 a.a. pore forming antibiotic, was given to permeabilize the IMM at the end of the protocol; a fall in PBFI fluorescence after alamethicin confirmed mK^+ influx in HL-1 cells. To quantify the mK^+ flux, the ΔPBFI ratio was determined as the increase in PBFI ratio during the initial 30 s after adding $CaCl_2$. ΔPBFI ratio =(p − b) / b where p = peak increase, and b=baseline before adding $CaCl_2$.

2.9. Hypoxic stress and cell damage with SK3.1 overexpression in HL-1 cells

HL-1 cells were plated on gelatin/fibronectin coated 35 mm dishes and transfected individually with pEGFP-N3, $SK3_{FL}$-EGFP, $SK3_{\Delta 1–277}$–EGFP and $SK3_{\Delta 626–720}$–EGFP for 48 h. Hypoxia was induced by placing cells in a culture medium containing glucose-free DMEM and 10 mM 2-deoxyglucose; culture dishes were then placed in an airtight chamber

in a 37 °C incubator and flushed with a hypoxic gas mixture of 95% N_2 + 5% CO_2. The cells were exposed to hypoxia for 2 h, after which the hypoxic medium was replaced by a reoxygenated DMEM medium containing 2% FBS at 37 °C with 95% air, +5% CO_2 (normoxia) for 2 h. For normoxia only (control), HL-1 cells were kept in normal DMEM medium containing 10% FBS with 95% air +5% CO_2 at 37 °C. After 2 h the medium was changed to DMEM with 2% FBS and the cells were cultured for another 2 h. To assess cell damage after 2 h reoxygenation, lactate dehydrogenase (LDH) release into the reoxygenated medium in hypoxic and normoxic dishes was measured using an LDH kit (Diagnostic Chemicals Limited, Oxford, CT, USA); data were expressed as percentage of EGFP normoxic controls (100%).

2.10. Silencing of SK3 with siRNA in HL-1 cells

To examine the effect of silencing of SK3 on HR injury, HL-1 cells were transfected with SK3 *Silencer*® *Select* siRNA duplexes or scrambled siRNA at concentrations of 5 nM using Lipofectamine RNAiMAX (Invitrogen), according to the manufacturer's instructions. Two *Silencer*® *Select* siRNAs for mouse *Kcnn3* (SK3) exon 1 and exon 4 were obtained (ThermoFisher Scientific). Transfection was performed in serum-free OptiMEM (Invitrogen) medium after which it was replaced with medium containing serum 4 h after transfection.

To confirm the silence of SK3 by siRNA in HL-1 cells, SK3 mRNA expression was measured with real time-qPCR. Total RNA was extracted from HL-1 cells transfected with SK3 siRNA or scramble siRNA using RNeasy mini kit (Qiagen, Crawley, UK). One μg of total RNA was used for cDNA synthesis with iScript cDNA synthesis kit (BioRad). SK3 mRNA expression was measured using SYBR Green Master mix (Bio-Rad). Primers specific for mouse gene *Kcnn3* designed to detect the sequence between exon 3 and exon 4 and given an amplicon of approximately 65 base pairs were purchased (ThermoFisher Scientific). Reactions were carried out in a Bio-Rad 7000 real-time thermocycler PCR machine using the following cycle conditions: 95 °C for 10 min, followed by 40 cycles at 95 °C for 15 s and 60 °C for 1min. Results were normalized to β-actin levels. See Supplemental materials, S.4 for silencing of SK3 in H9c2 cells.

2.11. Apoptotic cell death assay (TUNEL staining) after HR injury in SK3-silenced HL-1 cells

Apoptotic cell death was detected and quantified based on TUNEL assay (In Situ Cell Death Detection Kit, Roche) according to the manufacturer's protocol. In brief, HL-1 cells grown on glass coverslips (5 coverslips per group) were transfected with SK3 siRNA duplexes or scramble siRNA for 48 h (Section 2.10). To assess a possible role for SK3 in HR injury, HL-1 cells that were transfected with SK3 siRNA or scramble siRNA were exposed to normoxia (95% air + 5% CO_2) or to hypoxia (95% N_2 + 5% CO_2) for 2 h in a medium containing 2- deoxyglucose followed by 16 h reoxygenation (20% O_2 and 5% CO_2) with claycomb medium containing 10% FBS. Cells were washed with PBS and then fixed with 4% paraformaldehyde for 1 h at room temperature. Cells were permeabilized with 0.1% Triton X-100 for 10 min at room temperature followed by incubation with a TdT enzyme and nucleotide mixture for 1 h at 37 °C. After incubation, cell nuclei were stained with DAPI and the cells were imaged with a fluorescence microscope. Apoptotic cell death was

determined as a percentage of TUNEL-positive cells to the total number of cells. For each group, a total of approximately 2000 cells were counted. See Supplemental materials, S.5 for cell death in SK3-silenced H9c2 cells.

2.12. Mitochondrial membrane potential ($\Delta\Psi_m$) during simulated IR in SK3-silenced HL-1 cells

HL-1 cells were grown in glass bottom 35 mm dishes and transfected with SK3 siRNA duplexes described above (Section 2.10). After 48 h, cells were loaded with 10 nM TMRM (tetramethylrodamine methyl ester), a marker of $\Delta\Psi_m$, in Tyrode buffer for 30 min at 37 °C prior to simulated IR; all solutions contained 5 nM TMRM during recordings. The cell dish was assembled with closed perfusion cell culture dish inserts (Warner Instrument) for solution changes during recording and then mounted onto the stage of a confocal microscopy (Nikon A1R). TMRM fluorescence (λ_{em}552 nm and λ_{ex}543 nm) was first recorded in oxygenated Tyrode buffer for 6 min as baseline and then simulated ischemia was initiated by exchanging normal Tyrode buffer with a simulated ischemia buffer containing (in mM) 20 2-deoxyglucose, 2 NaCN, 135 NaCl, 4 KCl, 1 $MgCl_2$, 2 $CaCl_2$, and 10 Hepes, pH 6.4 [38,40] through the inlet and outlet ports of the perfusion cell culture dish inserts. After 10 min incubation in simulated ischemia buffer, restoration of the control conditions was initiated by suffusing the cells with normal Tyrode buffer through the cell culture dish inserts over 8 min to wash out the simulated ischemia buffer. Fluorescent images were acquired with an A1R confocal microscope using the NIS-elements AR software (Nikon) every 3 min during baseline and simulated IR. TMRM fluorescence intensity was analyzed off line using ImageJ. Results were expressed as changes in fluorescence intensity relative to baseline (=1).

2.13. Other methods

The following methods are described in Supplemental materials: S.1. Preparation of cardiac mitochondria and inner mitochondrial membrane and Western blotting; S.2. O_2 consumption in isolated cardiac mitochondria after global IR injury; S.3. IEM localization of SK3 channel protein in human cardiac mitochondria; S.4. Silencing of siRNA in H9c2 cells; S.5. Apoptotic cell death assay (TUNEL staining) in H9c2 cells; S.6. Mitochondrial membrane potential ($\Delta\Psi_m$) during simulated IR in H9c2 cells.

2.14. Statistical analyses of heart and mitochondrial data

Data obtained from hearts and mitochondria were expressed as means ± standard error of the means (SEM). Appropriate comparisons were made among groups that differed at a given condition or time, and within a group over time compared to the initial control data. Statistical differences were measured across heart groups using data collected before and after ischemia or in cells at given time points before or after hypoxia or simulated ischemia. Differences among variables were determined by two-way multiple ANOVA for repeated measures (Statview® and CLR Anova® software programs for Macintosh®); if F tests were significant, appropriate post-hoc tests (e.g., Student- Newman-Keuls) were used to compare means. Mean values were considered significant at P values (two-tailed) < 0.05.

3. Results

3.1. Cardiac effects of a SK_{Ca} channel agonist and an antagonist, and TBAP, after IR injury in guinea pig isolated hearts and in rat hearts in vivo

We tested effects of a SK_{Ca} channel agonist (DCEB), a SK_{Ca} antagonist (NS8593), and the mitochondria-targeted ROS scavenger TBAP *vs.* vehicle (IR control) on cardiac function (developed LVP) and damage (infarct size) in *ex vivo* guinea pig hearts, and infarct size in *in vivo* rat hearts. Unlike in our prior preconditioning study [14], in this study drugs were perfused continuously before, during and after ischemia. Developed LVP (Fig. 1A) was markedly reduced after 35 min no flow, global ischemia and 120 min reperfusion without drug treatment. NS8593 alone had no effect to worsen developed LVP. DCEB markedly improved LVP and this effect was reversed by NS8593. TBAP alone had no effect on LVP but completely blocked the protection afforded by DCEB. Like function, infarct size (Fig. 1B) was markedly reduced by DCEB alone, unaffected by NS8593, and the protection afforded by DCEB was blocked by either NS8593 or TBAP. Heart rate was not affected by any drug and was not different before ischemia or after 30 min reperfusion. At 10 min before ischemia, and at 30 and 120 min reperfusion, heart rates (beats/min) were, respectively, for TC: 245 ± 2, 244 ± 3, 246 ± 4; for IR only: 235 ± 2, 232 ± 3, 238 ± 4; for DCEB: 245 ± 2, 246 ± 4, 248 ± 5; and for NS8593: 236 ± 2, 240 ± 5, 242 ± 3 (± SEM; $P > 0.05$ between groups).

To test if DCEB and NS8593 had effects on the *in vivo* heart, rats were infused i.v. with DCEB, NS8593, or vehicle before and after LAD occlusion and infarct size (% ventricular area-at-risk) was assessed after 35 min of regional ischemia and 120 min reperfusion (Fig. 2). NS8593 significantly enhanced infarct size, whereas DCEB significantly reduced infarct size. These results highlight the functional significance and cardioprotective role of endogenous SK_{Ca} channels in rat hearts *in vivo*.

3.2. SK_{Ca} channel agonist improved mitochondrial respiration after IR injury

The results above showed the importance of cardiac SK_{Ca} at the organ (whole heart: *ex vivo* and *in vivo*) level. To further focus on the impact of SK_{Ca} at the mitochondrial level, we explored if the SK_{Ca} channel agonist DCEB protected and if the antagonist NS8593 impaired mitochondrial function after IR injury (Table 2, Fig. 3). We measured O_2 consumption and calculated respiratory control index (RCI) in guinea pig ventricular mitochondria that were isolated after 20 min reperfusion in isolated hearts treated with DCEB, NS8593, or vehicle before and after 35 min global ischemia. When using the complex I substrate pyruvate (Table 2, Fig. 3A), we found that IR ± NS8593, but not IR + DCEB treatment, increased states 2 and 4 respiration and decreased state 3 respiration compared to TC; RCI was markedly lower after IR ± NS8593 *vs.* TC. IR + DCEB decreased states 2 and 4 respiration and increased RCI and state 3 respiration *vs.* IR alone. With the complex II substrate succinate (Table 2, Fig. 3B), or with succinate plus rotenone, a complex I blocker (Table 2, Fig. 3C), state 3 respiration was slower after IR ± NS8593 but less slow after IR + DCEB, whereas state 4 respiration was faster after IR + DCEB. TC; RCI was lower after IR ± NS8593 and IR + DCEB, but IR + DCEB increased state 3 respiration and RCI *vs.* IR alone. The SK_{Ca} antagonist NS8593 exerted no significant effect on RCI from

the effect of IR alone. These results from isolated mitochondria confirm the functional contribution of cardiac SK_{Ca} channels in intact hearts, and circumstantial evidence ties the changes in mitochondrial respiration, at least in part, to mSK_{Ca} channel activation and inhibition.

3.3. Mitochondrial Ca^{2+}-induced K^+ uptake depended on Ca^{2+} uptake and mSK_{Ca} channel opening

We tested for mK^+ uptake via mSK_{Ca} channels when stimulated by mCa^{2+} uptake through the MCU and determined if the mK^+ uptake can be blocked by another mSK_{Ca} channel antagonist, UCL1684. Representative traces (Fig. 4A, B) and average of peak increases in mK^+ uptake recorded during the 250 to 260 s interval for each treatment group are shown (Fig. 4C). Increasing the amount of $CaCl_2$ added to the buffer increased the amount of mK^+ uptake over time (Fig. 4A, C); the highest mK^+ level tended to approach that elicited by the K^+ ionophore valinomycin. UCL1684 blocked mK^+ uptake whereas addition of cyclosporine A (CSA), an inhibitor of mPTP, did not alter mK^+ uptake, indicating the mPTP was not open (Fig. 4B, C). Blocking mCa^{2+} uptake through the MCU with Ru360 prevented mK^+ uptake; this indicates that the mSK_{Ca} channel Ca^{2+} sensor is probably located on the matrix side of the IMM.

3.4. Expression of SK3 splice variants in mitochondria of ventricular myocytes of different species

The pharmacological experiments suggest (Section 3.2) and support (Section 3.3) the functional relevance of mSK_{Ca} channels in heart mitochondria. To confirm mSK_{Ca} localization and its molecular identity we examined messenger RNA expression of the isoforms SK1, SK2, and SK3 in isolated guinea pig ventricular myocytes by RT-PCR using the specific primers listed in Table 1. SK2 and SK3, but not SK1, was amplified from guinea pig ventricular myocyte cDNA (Fig. 5A); this indicated that genes encoding SK2 and SK3 exist in guinea pig ventricular myocytes. In our previous report [14] we furnished initial evidence that SK_{Ca} channel isoforms SK2 and SK3 are expressed in guinea pig ventricular mitochondria. For this study we focused solely on the SK3 gene product. PCR fragments from lanes 5 and 6 (SK3) (Fig. 5A) were purified and sequenced. Red-labeled amino acids (a.a.) indicate the deduced a.a. sequences from the amplified genes (Fig. 5B). Sequence alignments indicated that the amplified SK3 was similar to the human SK3 named splice variant a (aka SK3-1) [41] which lacks the a.a. sequence ^{473}PESPARLSCSSFPAW^{487} that is present in the human canonical SK3 protein and designated as protein variant SK3c (aka SK3.2 (Fig. 5B). Thus, alternatively, the guinea pig sequence SK3.1 might be designated SK3a due to the missing P-W sequence and SK3c for the predicted sequence. No PCR product was obtained from templates generated in the absence of reverse transcriptase (Fig. 5A, Lane 11), thus confirming the absence of genomic contamination of the mRNA samples.

To further confirm the mitochondrial localization of SK3 in guinea pig heart, we examined the existence of SK3 protein in guinea pig heart, mitochondria and IMM by Western blot. Similar to the guinea pig heart, both cardiac mitochondria and IMM expressed SK3 at 75 kDa (Fig. 5C). Moreover, a 40 kDa band also displayed an intense response with the SK3 antibody; this suggested a truncated SK3 may also existent in mitochondria. To verify the

specificity of the SK3 bands reacting with the SK3 antibody, the anti-SK3 antibody was neutralized by preincubating it with a control antigen (immunizing peptide) before performing the Western blot. Indeed, both 75 and 40 kDa SK3 bands disappeared after the anti-SK3 was neutralized (Fig. 5C, anti-Sk3 preincubation panel). This furnished evidence that 75 and 40 kDa bands are SK3 specific, and that SK3 is expressed explicitly in guinea pig ventricular mitochondrial IMM.

We next examined for expression of SK3 splice variants in human ventricular tissue. First the mRNA expression of possible SK3 splice variants in human ventricular tissue was examined by RT-PCR. The primers were designed based on the identical a.a. sequences of guinea pig and human tissue. Lane 9 (Fig. 5A) shows that when using human SK3.1F1 and human SK3.1R1 primers corresponding to a.a. 1–6 and a.a. 340–346 in human (h) (a.a. 1–6 and a.a. 329–335 in guinea pig) there were several bands amplified, suggesting that the amplification for the SK3 segment, a.a. 1–346 was not specific. Lane 10 (Fig. 5A) demonstrates the one specific band ~1400 bp that was amplified from human ventricular tissue by a forward primer hSK3.1F2 that covered a.a. 280–286 for guinea pig and a.a. 290–296 for human (Methods, Section 2.5); the reverse primer hSK3.1R2 covered a.a. 714–720 for guinea pig and a.a. 725–731 for human (Methods, Section 2.5). This band was purified and sequenced. Human (h)SK3.1 and SK3.2 sequences (Fig. 5B) that are marked by red font show the deduced a.a. sequences from the sequenced band. Amino acid sequence alignments demonstrated hSK3.1 was nearly identical (> 97% homology) to the guinea pig SK3.1 with only one a.a. difference (a.a. 480) between the transmembrane 3 to the Ca^{2+} calmodulin binding domain (CaMBD) region; as noted above, hSK3.1 lacks the same a.a. sequence (^{484}P–W^{498}) attributed to the guinea pig SK3.2. The hSK3.2 isoform designated as splice variant 2, exhibits> 97% homology to the a.a. 295–714 sequence of guinea pig SK3.1, but also lacks ^{484}P–W^{498} of guinea pig SK3.2 and a large portion (~a.a. 1–294) of the N-terminus (Fig. 5B), which defines the gene product as SK3.2 [41]; but since it also lacks ^{484}P-W^{498} present in guinea pig SK3.3, this suggests that the canonical human and guinea pig SK3 include this sequence.

We then localized SK3 channels to mitochondria of human ventricular cells by visualizing immunogold labeled particles in isolated mitochondria with high resolution IEM (Fig. 6A). Shown are four mitochondria containing gold particles identified as SK3 channels; all scanned mitochondria were positive for immunogold. Negative controls (data not shown) (non-immune rabbit polyclonal serum) showed no gold particles in any field view (see also Supplemental materials, Fig. S1). Positive controls (labeling with antibody to COX 1) showed gold particles in mitochondria (data not shown). Moreover, Western blots show that mitochondria, specifically the IMM, displayed a higher level of expression of mSK3 at a band size of approximately 40 kDa compared to total human ventricular tissue (Fig. 6B).

DCEB provided protection against IR injury in rats *in vivo* (Fig. 2), so we examined if the SK3 channel is also located in mitochondria of rat isolated ventricular myocytes by using a double-labeled immunofluorescence staining technique i.e., anti-COX 1 antibody, a mitochondrial protein, for merging with anti-SK3 antibody. Confocal microscopic imaging and quantitative liner scan analyses displayed SK3 protein (Fig. 6C) as a longitudinal punctate label (SK3 panel) that co-localized with the COX 1 (complex IV) label (merged

panel, intensity panel), thereby showing expression of SK3 in the mitochondria of rat ventricular myocytes. Taken together, our data demonstrate that mSK3 channels are located in human, guinea pig, and rat ventricular mitochondria, and suggest that a hSK3.2 splice variant (but also missing the P-W sequence) is located in human cardiac mitochondria.

3.5. SK3.1-EGFP localized to mitochondria in HL-1 cells

We next sought to determine which domain of mSK3.1 (guinea pig) is important for mitochondrial trafficking. To do so, plasmids with fulllength SK3, $SK3_{FL}$-EGFP, N terminal truncated SK3, i.e. $SK3_{\Delta 1–277}$–EGFP or C terminal truncated SK3, i.e. $SK3_{\Delta 626–720}$–EGFP, were transfected into HL-1 cells. Two days after transfection cells were loaded with mitotracker red (MTR) and the location of expressed $SK3_{FL}$, $SK3_{\Delta 1–277}$ and $SK3_{\Delta 626–720}$ was examined using confocal microscopy (Fig. 7). EGFP fluorescence revealed the distribution of EGFP tagged $SK3_{FL}$ (Fig. 7A), $SK3_{\Delta 626–720}$ (Fig. 7B) and $SK3_{\Delta 1–277}$ (Fig. 7C) (green, left panels), and MTR displayed the mitochondrial pattern in HL-1 cells (Fig. 7A–C, red, middle panels). The graphs on the right side of each merge panel show the intensity profiles of two selected lines (regions 1 and 2), individually. The EGFP tagged proteins $SK3_{FL}$, $SK3_{\Delta 1–277}$ and $SK3_{\Delta 626–720}$ were expressed in a punctate, filamentous, and reticular pattern within regions of HL-1 cells. Merged images of EGFP fluorescence and MTR (Fig. 7A–C, merge panels and intensity panels) showed that $SK3_{FL}$ and $SK3_{\Delta 1–277}$, but not $SK3_{\Delta 626–720}$, partially co-localized with MTR, indicating mitochondrial localization of SK3.1. These results indicate that the C-terminus, exclusive of the CaMBD, and clearly not the N-terminus, likely plays a critical role in trafficking SK3.1 into mitochondria.

3.6. Overexpression of SK3.1 enhanced Ca^{2+}-activated K^+ uptake in HL-1 cells

Our pharmacological approach demonstrated the functional relevance of Ca^{2+}-induced activation of mSK_{Ca} channels to promote mK^+ uptake (Fig. 4). To provide further molecular evidence, we overexpressed SK3.1 and directly measured mK^+ uptake in HL-1 cells using the K^+-selective fluorescent indicator PBFI-AM as we showed previously [32]. To assess the uptake of K^+ into mitochondria, HL-1 cells were permeabilized with digitonin after dye loading but before adding KCl and $CaCl_2$ into the perfusion buffer (Fig. 8). The rate of mK^+ uptake was indicated by increased fluorescence after adding $CaCl_2$ to the buffer. We show (Fig. 8F) a summary of mitochondrial ΔPBFI ratio changes, as the index of mK^+ uptake, induced by adding $CaCl_2$ in HL-1 cells overexpressing EGFP, full length (FL) and 626–720 a.a. truncated (Δ626–720) SK3. In $SK3_{FL}$-EGFP overexpressed HL-1 cells, the rate of mK^+ uptake (Fig. 8A, F) after adding $CaCl_2$ was higher than that in only EGFP overexpressed HL-1 cells (Fig. 8C, F). To further confirm that $CaCl_2$-inducd K^+ uptake in $SK3_{FL}$-EGFP overexpressed HL-1 cells occurred in mitochondria, alamethicin was added to the perfusion buffer to permeabilize the IMM. After adding alamethicin, PBFI fluorescence fell immediately, indicating that K^+ was released from mitochondria (Fig. 8B).

In $SK3_{FL}$-EGFP overexpressed HL-1 cells, adding $CaCl_2$ increased mK^+ uptake (Fig. 8E, 1200 s); in contrast, adding apamin before adding $CaCl_2$ completely blocked mK^+ uptake (Fig. 8E and F, 2800 s); this indicated that the $CaCl_2$-induced increase in mK^+ was most likely due to enhanced opening of overexpressed SK3.1 channels. In addition, overexpression of $SK3_{FL}$-EGFP (Fig. 8A, B, E), but not the truncated $SK3_{\Delta 626–720}$-EGFP

(Fig. 8D, F), caused an increased rate of mK^+ uptake in HL-1 cells in response to added $CaCl_2$. This suggested that the distal C-terminus, the region beyond the end of CaMBD of mSK3.1, is required for Ca^{2+}-stimulated mK^+ uptake.

In addition to overexpressing SK3 protein to enhance $CaCl_2$-induced mK^+ uptake, we also tested if increased mK^+ uptake occurs when mSK_{Ca} channels are activated by DCEB. It has been reported that DCEB augments SK_{Ca} channel activity by increasing its apparent sensitivity to Ca^{2+} [18]; therefore, $CaCl_2$ was included in the experimental buffer. In digitonin permeabilized HL-1 cells, treatment with DCEB induced greater mK^+ uptake compared to no DCEB (Fig. S4, Supplemental materials); this indicated that mSK_{Ca} channels can be activated to increase mK^+ uptake by its pharmacological agonist.

3.7. Overexpression of SK3.1 protected HL-1 cells against hypoxia and reoxygenation injury

The functional results (Figs. 1-4) predicted that opening of mSK3.1 would be cytoprotective. So we examined next if SK3.1 channel overexpression improved cellular viability against 2 h hypoxia and 2 h reoxygenation (HR) injury in HL-1 cells. Cells were transiently transfected with pEGFP-N3 or EGFP-tagged $SK3_{FL}$, $SK3_{\Delta 1–277}$ or $SK3_{\Delta 626–720}$ plasmids and then subjected to HR. The relative increase in LDH release after HR was less in $SK3_{FL}$ and $SK3_{\Delta 1–277}$ than in EGFP and $SK3_{\Delta 626–720}$ transfected cells (105 ± 1%, 95 ± 0% *vs.* 157 ± 21%, 132 ± 26%, respectively, n =24 dishes, $P < 0.05$) (Fig. 9). This suggested that overexpression of SK3.1 channels in mitochondria protects cells against HR stress (Fig. 9) and that the protection requires the distal C-terminus beyond the CaMBD region of mSK3 (Fig. 8). These results in a cardiac cell line support the improved LVP and smaller infarct size in isolated *ex vivo* hearts (Fig. 1) and reduced infarct size *in vivo* hearts (Fig. 2) after DCEB treatment. The results are also consistent with the Ca^{2+}-activated mK^+ uptake (Figs. 8, 9) because the distal C terminal region (a.a. 626–720) is required to form an active tetramer [42].

3.8. Silencing of SK3 enhanced damage to HL-1 cells induced by hypoxia and reoxygenation

In contrast to overexpression of SK3.1, we next tested if knockdown of SK3.1 would exacerbate cell damage after oxidative stress. We knocked down SK3 by *silencer select* siRNA to SK3 exon 1 and exon 4 in HL-1 cells to assess the role of endogenous SK3 in protecting cells from HR injury. We found that SK3 mRNA expression was significantly decreased in cells treated with SK3 *silencer select* siRNA (24 ± 3%) compared to cells treated with scramble siRNA (100 ± 12%) (Fig. 10A). Cell death was assessed by the TUNEL assay. During normoxia, knockdown of SK3 in HL-1 cells induced only limited apoptotic cell death (1.5 ± 0.4%) compared to the scramble nonsilencing control (0.66 ± 0.05%) (Fig. 10B, C). But HR further exacerbated apoptotic cell death by 26.0 ± 2.3% in the SK3 knockdown cells compared to the scramble cells (13.7 ± 1.7%) (Fig. 10B, C).

We explored further if knockdown of SK3 was linked directly to mitochondrial damage by examining the effects of short-term HR on $\Delta\Psi_m$ (TMRM fluorescence) in SK3 knockdown HL-1 cells using confocal microscopy (Fig. 11). We found that $\Delta\Psi_m$ slowly decreased in

both SK3 and scrambled siRNA transfected cells during 10 min hypoxia and 8 min reoxygenation (Fig. 11A, B). However, in the SK3 siRNA transfected cells there was a significantly greater decline in $\Delta\Psi_m$ than in scrambled siRNA transfected cells during HR (45 ± 3% *vs.* 78 ± 2% at 15 min, respectively) when compared to time controls (100%) (Fig. 11).

To verify that silencing of SK3 enhances the HR-induced cell damage in another cardiac cell line, we also silenced SK3 in H9c2 cells, a rat cardiac myoblast cell line, and examined for cell apoptosis induced by HR (Fig. S2, Supplemental materials) and for a decline in $\Delta\Psi_m$ induced by HR (Fig. S3, Supplemental materials). These results are consistence with the HL-1 cell data, suggesting that SK3 may protect against HR and IR-induced cell damage in mitochondria of other cardiomyocyte cell lines. The increase in cell death with silencing of SK3 during HR is also consistent with antagonism of SK_{Ca} channels by NS8593 to increase infarct size after regional IR in *in vivo* hearts (Fig. 2).

4. Discussion

In this report we show overall that endogenous and drug-induced opening of the SK_{Ca} channel reduces infarct size after IR injury *in vivo* and that the SK_{Ca} agonist DCEB improves contractility and reduces infarct size after IR injury in *ex vivo* and *in vivo* hearts. Additionally, we provide strong molecular evidence for the cardiac mSK_{Ca} channel in rat and human hearts that was identified in our earlier report in guinea pig hearts [14]. Moreover, we identify SK3.1 (alternatively known as SK3a) as the splice variant present in cardiac mitochondria of guinea pigs, and human SK3.2 as the probable splice variant present in cardiac mitochondria of humans. We found that overexpression of SK3.1 in HL-1 cells protects against HR injury. In contrast, silencing of SK3 enhances HR-induced cell death by damaging mitochondria. By overexpressing full length and N and C terminal truncated SK3.1, we established that the C-terminus downstream of CaMBD is required for SK3.1 expression in mitochondria, and that mK^+ uptake is activated by an increase in mCa^{2+} that first binds to mitochondrial calmodulin [43] to initiate mK^+ uptake. Together, the molecular and physiological results support a prominent role of mSK_{Ca} channels in mitochondria and cardiac protection during IR or HR injury.

4.1. SK_{Ca} channel agonists/antagonists infer cardio-protective and antiprotective effects of K_{Ca} channels

Our isolated heart study (Fig. 1) supports our earlier report that pharmacological pre-conditioning by DCEB or NS1619 [14,16] leads to an essential intermediate step, $O_2\cdot^-$ generation, in eliciting cardioprotection. Unlike for the $\Delta\Psi_m$-dependent BK_{Ca} channel opening, the SK_{Ca} channel opening could be important under conditions in which $\Delta\Psi_m$ is reduced during oxidative stress and when $m[Ca^{2+}]$ is high. Importantly, when infused i.v., DCEB and NS8593 produced a decrease and an increase, respectively, in infarct size after LAD occlusion in intact rats (Fig. 2), thus extending what we found in the *ex vivo* guinea pig IR model. These *in vivo* results suggest a translational appeal for i.v. treatment of a SK_{Ca} channel agonist in ischemic heart disease. Pharmacological evidence for a role of the SK_{Ca} channel in mitochondrial protection was suggested by the improved RCIs (Fig. 3) in isolated

guinea pig mitochondria after IR injury of hearts treated with DCEB. The observation that graded increases in m[Ca^{2+}] induce graded increases in mK^+ influx that were blocked by SK_{Ca} channel blocker UCL 1684 furnished direct evidence for Ca^{2+}-induced mK^+ uptake via mSK_{Ca} channels (Fig. 4).

We furnish novel evidence that the site of the Ca^{2+} sensor is intramitochondrial because of the lack of an increase in mK^+ flux when Ru360 was used to block the MCU (Fig. 4). This is likely the first evidence that provides insight into the orientation of SK_{Ca} channels in mitochondria. That the cardioprotection is mediated at the mitochondrial level is also supported by the effect of the mitochondria-targeted ROS scavenger, TBAP, since mitochondria are the major source of cell ROS production during cardiac IR injury (Fig. 1). The importance of cardiac mSK_{Ca} channel opening in cardioprotection warranted further molecular examination.

4.2. Mitochondrial localization and function of small conductance Ca^{2+}-activated K^+ channels

The SK_{Ca} channels family consists of three isoforms SK1 ($K_{Ca}2.1$, *Kcnn1*), SK2 ($K_{Ca}2.2$, *Kcnn2*) and SK3 ($K_{Ca}2.3$, *Kcnn3*) [44]. These three isoforms display differential distribution in the heart. Previous reports [11,12,42] showed that SK3 was expressed at similar low levels in atria and in ventricles while SK1 and SK2 were significantly more abundant in atria. The presence of an apamin sensitive Ca^{2+}-activated K^+ current, i.e. SK2, was reported earlier [11,12,42] in the sarcolemma of mouse and human cardiomyocytes; but SK3 was expressed subcellular in mouse cardiomyocytes. We were the first to report the expression and function of SK2 and SK3 channel isoforms in mitochondria of cardiomyocytes [14]. In addition, SK2 was found recently to localize in the IMM of neuronal HT-22 cells, where SK2 activation by CyPPA attenuated mitochondrial fragmentation, prevented loss of $\Delta\Psi_m$, blocked lipid peroxidation, and reduced ROS production when cells were exposed to glutamate [25].

Based on our previous findings [14], we have extended our present study to further identify and characterize SK3 in cardiomyocyte IMM in other mammals and to search for the specifically expressed splice variant. In support of our prior evidence for SK3 protein in guinea pig ventricular mitochondria [14], in this study we provide additional evidence of SK3 channels locally expressed in mitochondria of rat and human ventricular myocytes (Fig. 6A–C). We further characterized the SK3 channel splice variant in guinea pig cardiac mitochondria and in human ventricular mitochondria by amplifying the SK3 gene using RTPCR. After deducing the a.a. sequence from the amplified SK3 nucleotide sequence we found that the identified guinea pig SK3 channel was splice variant 1 (SK3.1) (Fig. 5A, B). We also determined that for the human ventricular mitochondrial SK3, the likely splice variant is 2, i.e. SK3.2, which is an N-terminal truncated variant of human SK3 (Fig. 5A, B).

Mitochondrial localization of SK3 and splice variant SK3.1 is supported by our pharmacological and molecular evidence: a) the higher respiration rate in mitochondria from hearts treated with DCEB before and after IR compared to IR alone (Fig. 3); b) the presence in guinea pig cardiac IMM of SK3 proteins at 75 and 40 kDa by Western blots, which disappeared after treating SK3 antibody with the control antigen (Fig. 5C); c) SK3

immunogold labeling of isolated human ventricular mitochondria (Fig. 6A); d) higher human SK3.2 expression in mitochondria than in total ventricular lysate (Fig. 6B); e) SK3 colocalization with mitochondrial protein COX 1 in isolated rat cardiomyocytes (Fig. 6C); f) SK3 partially colocalizing in mitochondria when SK3 was overexpressed in HL-1 cells (Fig. 7); and greater apoptosis (Fig. 10) and mitochondrial depolarization (Fig. 11) after silencing of SK3 during hypoxia/simulated ischemia of HL-1 cells.

Our finding that SK3.1 locates within the IMM of ventricular myocytes is consistent with the report of Fay et al. [45] that SK3 affects mitochondria ROS production in neutrophils. But in a report by Tuteja et al. [42], three isoforms of SK channels were found distributed along the Z-lines in atrial myocytes with no observation of their location in mitochondria. The difference between our results and those of Tuteja et al. [12,42] may be related to the technique of permeabilization and immunostaining of SK channels in cardiomyocytes; moreover, Western blot analysis is more sensitive than cell immunostaining.

4.3. Requirement of C-terminus of SK3.1 for mitochondrial trafficking and Ca^{2+}-activated K^+ uptake

We have shown that SK3 localizes to mitochondria of human, rat, and guinea pig cardiomyocytes. However, it is important to know how SK3 localizes to mitochondria, and which domain is important for trafficking and channel function. The functional SK_{Ca} channel is a tetramer; Ca^{2+} sensitivity is conferred via the CaMBD in the C-terminus [46]. Correct refolding, assembly, and trafficking are required for SK_{Ca} channel function. In rat neuronal PC12 cells, deletion of the distal Cterminus reduced cell surface expression of SK3 by 75%, whereas truncated SK3 channels were blocked from leaving the endoplasmic reticulum to migrate to the Golgi; this suggested that a region downstream of the CaMBD region, i.e. the distal C-terminus, is required for SK3 to traffic into the Golgi [47]. Deletion of the distal C-terminus (leucine zipper region) of the human SK4 isoform was reported to prevent SK4 from trafficking to the cell surface and to block channel function because of improper refolding and assembly [48,49]. Moreover, SK3 units assemble in homo-tetrameric as well as in heteromultimeric complexes with SK1 and SK2 via the coiled-coil domains in the distal C-terminus of these channels [42]; this suggests that the Cterminus is an important molecular determinant for SK3 trafficking and channel function. Our results (Fig. 8) showed that the guinea pig truncated $SK3_{\Delta 626–720}$ failed to traffic to mitochondria, whereas the Nterminus truncated $SK3_{\Delta 1–277}$ localized to mitochondria where it increased Ca^{2+}-activated mK^+ uptake. This indicated that the Cterminus is required both for SK3 trafficking to mitochondria and for Ca^{2+}-induced mK^+ activation, which is consistent with previous reports [42,47].

Like the C-terminus, the N-terminus of the SK_{Ca} channel is highly conserved over mammalian species but with some variations. The Nterminal a.a. sequence of SK3 displays 97% homology between human and guinea pig (Fig. 5B), but the guinea pig SK3 sequence has one short Q region and the human SK3 has two short Q regions. A prior report showed that the S1 segment, a.a. 274–299 of rat SK3, but not the sequence a.a. 1–274 contained peptides that might stabilize SK3 functional conformation and nuclear localization [50]. Truncation of the region before the S1 segment, as in our construct $SK3_{\Delta 1–277}$–EGFP (Figs.

7, 8), did not change SK3 functional conformation [51]. An electrophysiological study in PC-12 cells showed that expression of a.a. 1–299 SK3 did not affect Ca^{2+}-sensitivity or the number of endogenous SK3 functional channels, but did reduce sensitivity to the agonist 1-EBIO [50]. Moreover, a molecular determinant study in neuronal cells indicated that deletion of N-terminal domain a.a. 1–271 before the S1 segment caused SK3 to be retained in the ER while the truncated SK3 could assemble with wild type SK3 [47]. Therefore, the N-terminal domain of human SK3 may contain information relevant for channel trafficking and delivery to the plasma membrane, but not necessarily for SK3 channel assembly [47].

Our results (Fig. 8) also demonstrate that truncating the N-terminus a.a. 1–277 before the S1 segment did not affect SK3 Ca^{2+} sensitivity; this also agrees with prior studies [47,50]. Moreover, our results demonstrate that the N-terminal truncated SK3 can be expressed in mitochondria, which supports the findings of Frei et al. [50], but not those of Roncarati et al. [47]. The difference from the latter report [47] may arise because the N-terminus truncated SK3 can assemble with endogenous SK3 to form functional tetrameric channels that traffic to mitochondria. Also, the position of the mitochondrial localization signal is likely different from the cell membrane and nuclear membrane localization signals. Therefore, it is interesting that in our study the Nterminus had no effect on the mSK_{Ca} trafficking to mitochondria. This contrasts with the role of the N-terminus as a necessary component for trafficking to the plasma membrane. Though we did not identify the mitochondrial targeting sequence, it appears highly likely that region distal from the N-terminus is required.

4.4. Mechanisms of protection by mitochondrial SK_{Ca} channels against IR or HR stress

The presence of SK3.1 channels in the IMM may indicate that they have an important function in fine-tuning mitochondrial bioenergetics in response to a high cytosolic Ca^{2+}-induced rise in mCa^{2+}, perhaps via volume control, which is largely controlled by K^+ flux, or by an uncoupling effect [32] due to mKHE. It could be that SK_{Ca} channels are activated under ischemic conditions when $\Delta\Psi_m$ and pH_m are low. This would be in contrast to the voltage and Ca^{2+}-dependent BK_{Ca} channels that may open primarily during reperfusion when $\Delta\Psi_m$ and pH_m are high (state 4 respiration) and when there is an abrupt, large increase in cytosolic $[Ca^{2+}]$. This notion is consistent with how BK_{Ca} channels can modulate cell membrane potential in excitable cells.

Since SK_{Ca} channels are expressed in the cell membrane of many cell types [8], how they alter function at these sites may aid in understanding their mechanism of function in mitochondria. For example, SK3 activation reduced atrial fibrillation and ventricular arrhythmia [44], and electrophysiology experiments showed that overexpression of SK3 shortened the atrial action potential duration (APD) while knockdown of SK3 prolonged the APD [52]. Thus effects of SK3 channel activation on mK^+ uptake would be expected to alter mitochondria bioenergetics because of its effects on IMM ion homeostasis. A role of SK3 to retard cell death has been reported in some cancer and neuronal cells. For example, in the cancer cell line MDA-MB-231, which expresses SK3 but not SK2, inhibition of SK3 with NS8593, or knockdown of SK3 by siRNA, had a profound cytotoxic effect on cell viability [53]. In CNS-derived cell lines that express SK1, 2 or 3 channels, activation of SK channels with CyPPA ameliorated saturosporineinduced cell apoptosis [53].

The effects of overexpressing or silencing of SK3.1 (Figs. 8-11) to alter the viability of cardiomyocytes likely occur through mitochondrial pathways induced by IR or HR injury. Our data in intact hearts and isolated mitochondria are consistent with those obtained in the MDAMB- 213 cancer cells [53]. Although unknown, it is possible that SK_{Ca} channels play an important role in protecting cancer cells from oxidative injury by a mitochondrial mediated mechanism. Our results demonstrate that SK3 knockdown increases apoptosis of myocytes, and that SK3 overexpression reduces LDH release induced by HR stress. Thus SK_{Ca} channel agonists and antagonists may be important adjuncts for therapeutic interventions in ischemic heart disease [44] and cancer [53], respectively. The SK3 knockdown effect and the *in vivo* rat model with infused i.v. SK_{Ca} antagonist NS8593 suggested endogenous protection in cardiomyocytes However, NS8593 did not worsen LVP or enhance infarct size significantly in the isolated heart model, in contrast to the *in vivo* and cell line results. We used rats for the *in vivo* model and HL-1 cells derived from mouse for the cell model, but for the isolated heart model we used guinea pigs. Possibilities for the difference may be due to different animal species, differential antagonism by NS8593, or different intracellular [Ca^{2+}] during *in vivo* regional IR *vs*. IR in the non-volume ejecting isolated heart. NS8593 is a negative allosteric modulator of SK_{Ca} channels that inhibits SK_{Ca} channels by decreasing their sensitivity to Ca^{2+} rather than by blocking the pore [54]. Such a compound has a bell-shaped inhibitory effect on SK_{Ca} channel current [54]. The IC_{50} of 3 μM NS8593 is approximately at 500–600 nM [Ca^{2+}] [54]. Therefore, the lack of statistical evidence for protection by endogenous SK3 channel opening in the *ex vivo* heart could be due to insufficient antagonism by NS8593 in that model.

Nevertheless, the mechanistic pathway of SK3 mediated protection against IR or HR induced cell dysfunction and apoptosis remains unclear. During oxidative stress mitochondria are a major source of excess ROS production [24]. However, there is now ample evidence that a small amount of triggering $O_2\cdot^-$ is necessary to mediate protection by mK^+ channel opening in the heart [14,16,24,55-57]. Our results (Fig. 1) confirm that the ROS scavenger TBAP abolishes BK_{Ca} [16] or SK_{Ca} [14] mediated cardioprotection in IR injury. Fay et al. [45] used human neutrophils and granulocyte-differentiated PLB-985 cells to show that activation of SK3 channels with 1-EBIO increased $O_2\cdot^-$ and H_2O_2 production in mitochondria without altering $\Delta\Psi_m$; this suggested that SK3 activation induced signaling ROS production. Therefore, SK3 channel opening by DCEB or SK3 overexpression could provide protection by inducing signaling $O_2\cdot^-$, which then stimulates downstream pathways that help to protect the cells from IR injury.

In isolated cardiac mitochondria we reported previously that the BK_{Ca} channel opener NS1619 could increase resting state 4 respiration and ROS generation while maintaining $\Delta\Psi_m$ [58]. Unlike our prior study on SK_{Ca} channel opening during PPC [14], in the current study the SK_{Ca} channel agonists were given before, during, and after ischemia; but this protocol would still trigger ROS production similar to a preconditioning effect. However, how activation of mSK_{Ca} induces the signaling ROS production in mitochondria is unclear. We have suggested [32] that an increase in $m[K^+]$ is replaced immediately with an increase in $m[H^+]$ via mKHE as K^+ is extruded. We proposed that at low concentrations, these K^+ channel openers cause a transient increase in matrix acidity, i.e., via a proton leak through

mKHE that stimulates respiration to maintain $\Delta\Psi_m$, but at a cost of increased $O_2\cdot^-$ generation due to electron leak at the respiratory complexes.

In addition to the signaling generation of ROS, an improvement in mitochondrial efficiency and reduction of m[Ca^{2+}] load may play an important role in triggering protection by mK^+ channel opening. For the K_{ATP} channel, it was proposed that its opening depolarizes the IMM to cause uncoupling and hasten respiration [59-61]. Subsequent ischemia would then reduce the driving force for Ca^{2+} influx via the MCU; this could attenuate mCa^{2+} overload [62,63] so that energized mitochondria on reperfusion would perform more efficiently. The end result of mSK_{Ca} channel opening, like any mK^+ channel opening, may be improved mitochondrial efficiency and reduced excess m[Ca^{2+}] and ROS production, thereby contributing to overall protection of mitochondrial function during IR.

4.5. Summary

We have furnished novel evidence for the presence of mSK_{Ca} channels in guinea pig, rat, and human ventricular myocyte mitochondria, and specifically, for the location of splice variant SK3.1 and SK3.2 in guinea pig and human mitochondria, respectively. We found that the C-terminus distal to the CaMBD is likely required both for trafficking to mitochondria and for channel function, whereas the N-terminus appears not to be required for trafficking to mitochondria or for channel activity. Ca^{2+} sensing for the mSK_{Ca} channel appears to occur in the matrix rather than in the cytosol. Overexpression or silencing of SK3 in cardiac-like cell lines results in less or more damage after stress injury, respectively. Activation of each type of mK^+ channel may converge on a pathway that stimulates a small amount of signaling ROS necessary to trigger activation of cardioprotective pathways. Thus the individual stages of triggering, activation, and end-effect must be well delineated to unravel the apparently complicated mechanism underlying cardiac protection, and specifically by the mSK_{Ca} channels.

Supplementary Material

Refer to Web version on PubMed Central for supplementary material.

Acknowledgments

The authors thank James S. Heisner, Ashish Gadicherla, Clive Wells, and Glen R. Slocum for their valuable contributions to this research study, which was supported in part by the Veterans Administration (BX- 002539-01) and the National Institutes of Health (P01-GM066730).

References

1. Singh S, Syme CA, Singh AK, Devor DC, Bridges RJ. Benzimidazolone activators of chloride secretion: potential therapeutics for cystic fibrosis and chronic obstructive pulmonary disease. J Pharmacol Exp Ther. 2001; 296:600–611. [PubMed: 11160649]
2. Stocker M. Ca^{2+}-activated K^+ channels: molecular determinants and function of the SK family. Nat Rev Neurosci. 2004; 5:758–770. [PubMed: 15378036]
3. Syme CA, Gerlach AC, Singh AK, Devor DC. Pharmacological activation of cloned intermediate- and small- conductance Ca^{2+}-activated K^+ channels. Am J Physiol Cell Physiol. 2000; 278:C570–C581. [PubMed: 10712246]

4. Wulff H, Miller MJ, Haensel W, Grissmer S, Cahalan MD, Chandy KG. Design of a potent and selective inhibitor of the intermediate-conductance Ca^{2+}-activated K^+ channel, IKCa1: a potential immunosupressant. PNAS. 2000; 97:8151–8156. [PubMed: 10884437]
5. Hille, B. Ion Channels in Excitable Membranes. third ed. Sinauer Asociates, Inc.; Sunderland: 2001.
6. Schumacher MA, Rivard AF, Bachinger HP, Adelman JP. Structure of the gating domain of a Ca^{2+}-activated K^+ channel complexed with Ca^{2+}/calmodulin. Nature. 2001; 410:1120–1124. [PubMed: 11323678]
7. Bruening-Wright A, Schumacher MA, Adelman JP, Maylie J. Localization of the activation gate for small conductance Ca^{2+}-activated K^+ channels. J Neurosci. 2002; 22:6499–6506. [PubMed: 12151529]
8. Wei AD, Gutman GA, Aldrich R, Chandy KG, Grissmer S, Wulff H. International Union of Pharmacology. LII. Nomenclature and molecular relationships of calcium-activated potassium channels. Pharmacol Rev. 2005; 57:463–472. [PubMed: 16382103]
9. Taylor MS, Bonev AD, Gross TP, Eckman DM, Brayden JE, Bond CT, Adelman JP, Nelson MT. Altered expression of small-conductance Ca^{2+}-activated K^+ (SK3) channels modulates arterial tone and blood pressure. Circ Res. 2003; 93:124–131. [PubMed: 12805243]
10. Yang Q, Huang JH, Man YB, Yao XQ, He GW. Use of intermediate/small conductance calcium-activated potassium-channel activator for endothelial protection. J Thorac Cardiovasc Surg. 2011; 141:501–510 (510 e501). [PubMed: 20546794]
11. Xu Y, Tuteja D, Zhang Z, Xu D, Zhang Y, Rodriguez J, Nie L, Tuxson HR, Young JN, Glatter KA, Vazquez AE, Yamoah EN, Chiamvimonvat N. Molecular identification and functional roles of a Ca^{2+}-activated K^+ channel in human and mouse hearts. J Biol Chem. 2003; 278:49085–49094. [PubMed: 13679367]
12. Tuteja D, Xu D, Timofeyev V, Lu L, Sharma D, Zhang Z, Xu Y, Nie L, Vazquez AE, Young JN, Glatter KA, Chiamvimonvat N. Differential expression of small-conductance Ca^{2+}-activated K^+ channels SK1, SK2, and SK3 in mouse atrial and ventricular myocytes. Am J Physiol Heart Circ Physiol. 2005; 289:H2714–H2723. [PubMed: 16055520]
13. Weatherall KL, Seutin V, Liegeois JF, Marrion NV. Crucial role of a shared extracellular loop in apamin sensitivity and maintenance of pore shape of smallconductance calcium-activated potassium (SK) channels. Proc Natl Acad Sci U S A. 2011; 108:18494–18499. [PubMed: 22025703]
14. Stowe DF, Gadicherla AK, Zhou Y, Aldakkak M, Cheng Q, Kwok WM, Jiang MT, Heisner JS, Yang M, Camara AK. Protection against cardiac injury by small Ca^{2+}-sensitive K^+ channels identified in guinea pig cardiac inner mitochondrial membrane. Biochim Biophys Acta. 2013; 1828:427–442. [PubMed: 22982251]
15. Xu W, Liu Y, Wang S, McDonald T, Van Eyk JE, Sidor A, O'Rourke B. Cytoprotective role of Ca^{2+}-activated K^+ channels in the cardiac inner mitochondrial membrane. Science. 2002; 298:1029–1033. [PubMed: 12411707]
16. Stowe DF, Aldakkak M, Camara AK, Riess ML, Heinen A, Varadarajan SG, Jiang MT. Cardiac mitochondrial preconditioning by Big Ca^{2+}-sensitive K^+ channel opening requires superoxide radical generation. Am J Physiol Heart Circ Physiol. 2006; 290:H434–H440. [PubMed: 16126810]
17. Sheng JZ, Ella S, Davis MJ, Hill MA, Braun AP. Openers of SK_{Ca} and IK_{Ca} channels enhance agonist-evoked endothelial nitric oxide synthesis and arteriolar vasodilation. FASEB J. 2009; 23:1138–1145. [PubMed: 19074509]
18. Pedarzani P, McCutcheon JE, Rogge G, Jensen BS, Christophersen P, Hougaard C, Strobaek D, Stocker M. Specific enhancement of SK channel activity selectively potentiates the afterhyperpolarizing current I(AHP) and modulates the firing properties of hippocampal pyramidal neurons. J Biol Chem. 2005; 280:41404–41411. [PubMed: 16239218]
19. Pedarzani P, Stocker M. Molecular and cellular basis of small- and intermediateconductance, calcium-activated potassium channel function in the brain. Cell Mol Life Sci. 2008; 65:3196–3217. [PubMed: 18597044]
20. Strobaek D, Teuber L, Jorgensen TD, Ahring PK, Kjaer K, Hansen RS, Olesen SP, Christophersen P, Skaaning-Jensen B. Activation of human IK and SK Ca^{2+}-activated K^+ channels by NS309

(6,7-dichloro-1H-indole-2,3-dione 3-oxime). Biochim Biophys Acta. 2004; 1665:1–5. [PubMed: 15471565]

21. Wulff H, Kolski-Andreaco A, Sankaranarayanan A, Sabatier JM, Shakkottai V. Modulators of small- and intermediate-conductance calcium-activated potassium channels and their therapeutic indications. Curr Med Chem. 2007; 14:1437–1457. [PubMed: 17584055]
22. Diness JG, Sorensen US, Nissen JD, Al-Shahib B, Jespersen T, Grunnet M, Hansen RS. Inhibition of small-conductance Ca^{2+}-activated K^+ channels terminates and protects against atrial fibrillation. Circ Arrhythm Electrophysiol. 2010; 3:380–390. [PubMed: 20562443]
23. Jenkins DP, Strobaek D, Hougaard C, Jensen ML, Hummel R, Sorensen US, Christophersen P, Wulff H. Negative gating modulation by (*R*)-*N*-(benzimidazol-2-yl)-1,2,3,4-tetrahydro-1-naphthylamine (NS8593) depends on residues in the inner pore vestibule: pharmacological evidence of deep-pore gating of $K_{Ca}2$ channels. Mol Pharmacol. 2011; 79:899–909. [PubMed: 21363929]
24. Stowe DF, Camara AK. Mitochondrial reactive oxygen species production in excitable cells: modulators of mitochondrial and cell function. Antioxid Redox Signal. 2009; 11:1373–1414. [PubMed: 19187004]
25. Dolga AM, Netter MF, Perocchi F, Doti N, Meissner L, Tobaben S, Grohm J, Zischka H, Plesnila N, Decher N, Culmsee C. Mitochondrial small conductance SK2 channels prevent glutamate-induced oxytosis and mitochondrial dysfunction. J Biol Chem. 2013; 288:10792–10804. [PubMed: 23430260]
26. Varadarajan SG, An JZ, Novalija E, Smart SC, Stowe DF. Changes in $[Na^+]_i$, compartmental $[Ca^{2+}]$, and NADH with dysfunction after global ischemia in intact hearts. Am J Physiol Heart Circ Physiol. 2001; 280:H280–H293. [PubMed: 11123243]
27. Kevin L, Camara AKS, Riess MR, Novalija E, Stowe DF. Ischemic preconditioning alters real-time measure of O_2 radicals in intact hearts with ischemia and reperfusion. Am J Physiol Heart Circ Physiol. 2003; 284:H566–H574. [PubMed: 12414448]
28. Kevin L, Novalija E, Riess MR, Camara AKS, Rhodes SS, Stowe DF. Sevoflurane exposure generates superoxide but leads to decreased superoxide during ischemia and reperfusion in isolated hearts. Anesth Analg. 2003; 96:945–959.
29. Riess ML, Camara AK, Novalija E, Chen Q, Rhodes SS, Stowe DF. Anesthetic preconditioning attenuates mitochondrial Ca^{2+} overload during ischemia in guinea pig intact hearts: reversal by 5-hydroxydecanoic acid. Anesth Analg. 2002; 95:1540–1546. [PubMed: 12456413]
30. An JZ, Camara AK, Rhodes SS, Riess ML, Stowe DF. Warm ischemic preconditioning improves mitochondrial redox balance during and after mild hypothermic ischemia in guinea pig isolated hearts. Am J Physiol Heart Circ Physiol. 2005; 288:H2620–H2627. [PubMed: 15653757]
31. Faulkner KM, Liochev SI, Fridovich I. Stable Mn(III) porphyrins mimic superoxide dismutase in vitro and substitute for it in vivo. J Biol Chem. 1994; 269:23471–23476. [PubMed: 8089112]
32. Aldakkak M, Stowe DF, Cheng Q, Kwok WM, Camara AK. Mitochondrial matrix K^+ flux independent of large-conductance Ca^{2+}-activated K^+ channel opening. Am J Physiol Cell Physiol. 2010; 298:C530–C541. [PubMed: 20053924]
33. Boelens AD, Pradhan RK, Blomeyer CA, Camara AK, Dash RK, Stowe DF. Extra-matrix Mg^{2+} limits Ca^{2+} uptake and modulates Ca^{2+} uptake-independent respiration and redox state in cardiac isolated mitochondria. J Bioenerg Biomembr. 2013; 45:203–218. [PubMed: 23456198]
34. Blomeyer CA, Bazil JN, Stowe DF, Dash RK, Camara AK. Mg^{2+} differentially regulates two modes of mitochondrial Ca^{2+} uptake in isolated cardiac mitochondria: implications for mitochondrial Ca^{2+} sequestration. J Bioenerg Biomembr. 2016; 48:175–188. [PubMed: 26815005]
35. Blomeyer CA, Bazil JN, Stowe DF, Pradhan RK, Dash RK, Camara AK. Dynamic buffering of mitochondrial Ca^{2+} during Ca^{2+} uptake and Na^+-induced Ca^{2+} release. J Bioenerg Biomembr. 2013; 45:189–202. [PubMed: 23225099]
36. Dunn PM. UCL 1684: a potent blocker of Ca^{2+}-activated K^+ channels in rat adrenal chromaffin cells in culture. Eur J Pharmacol. 1999; 368:119–123. [PubMed: 10096777]
37. Camara AK, Begic Z, Kwok WM, Bosnjak ZJ. Differential modulation of the cardiac L- and T-type calcium channel currents by isoflurane. Anesthesiology. 2001; 95:515–524. [PubMed: 11506128]

38. Sedlic F, Muravyeva M, Sepac A, Sedlic M, Williams AM, Yang M, Bai X, Bosnjak ZJ. Targeted modification of mitochondrial ROS production converts high glucose-induced cytotoxicity to cytoproteition: effects on anesthetic preconditioning. J Cell Physiol. 2016
39. Kozoriz MG, Church J, Ozog MA, Naus CC, Krebs C. Temporary sequestration of potassium by mitochondria in astrocytes. J Biol Chem. 2010; 285:31107–31119. [PubMed: 20667836]
40. Seidlmayer LK, Juettner VV, Kettlewell S, Pavlov EV, Blatter LA, Dedkova EN. Distinct mPTP activation mechanisms in ischaemia-reperfusion: contributions of Ca^{2+} ROS, pH, and inorganic polyphosphate. Cardiovasc Res. 2015; 106:237–248. [PubMed: 25742913]
41. Ohya S, Morohashi Y, Muraki K, Tomita T, Watanabe M, Iwatsubo T, Imaizumi Y. Molecular cloning and expression of the novel splice variants of K^+ channel-interacting protein 2. Biochem Biophys Res Commun. 2001; 282:96–102. [PubMed: 11263977]
42. Tuteja D, Rafizadeh S, Timofeyev V, Wang S, Zhang Z, Li N, Mateo RK, Singapuri A, Young JN, Knowlton AA, Chiamvimonvat N. Cardiac small conductance Ca^{2+}-activated K^+ channel subunits form heteromultimers via the coiled-coil domains in the C termini of the channels. Circ Res. 2010; 107:851–859. [PubMed: 20689065]
43. Hatase O, Doi A, Itano T, Matsui H, Ohmura Y. A direct evidence of the localization of mitochondrial calmodulin. Biochem Biophys Res Commun. 1985; 132:63–66. [PubMed: 3904750]
44. Clements RT, Terentyev D, Sellke FW. Ca^{2+}-activated K^+ channels as therapeutic targets for myocardial and vascular protection. Circ J. 2015; 79:455–462. [PubMed: 25746520]
45. Fay AJ, Qian X, Jan YN, Jan LY. SK channels mediate NADPH oxidase-independent reactive oxygen species production and apoptosis in granulocytes. Proc Natl Acad Sci U S A. 2006; 103:17548–17553. [PubMed: 17085590]
46. Xia XM, Fakler B, Rivard A, Wayman G, Johnson-Pais T, Keen JE, Ishii T, Hirschberg B, Bond CT, Lutsenko S, Maylie J, Adelman JP. Mechanism of calcium gating in small-conductance calcium-activated potassium channels. Nature. 1998; 395:503–507. [PubMed: 9774106]
47. Roncarati R, Decimo I, Fumagalli G. Assembly and trafficking of human small conductance Ca^{2+}-activated K^+ channel SK3 are governed by different molecular domains. Mol Cell Neurosci. 2005; 28:314–325. [PubMed: 15691712]
48. Khanna R, Chang MC, Joiner WJ, Kaczmarek LK, Schlichter LC. hSK4/hIK1, a calmodulin-binding K_{Ca} channel in human T lymphocytes. Roles in proliferation and volume regulation. J Biol Chem. 1999; 274:14838–14849. [PubMed: 10329683]
49. Joiner WJ, Khanna R, Schlichter LC, Kaczmarek LK. Calmodulin regulates assembly and trafficking of SK4/IK1 Ca^{2+}-activated K^+ channels. J Biol Chem. 2001; 276:37980–37985. [PubMed: 11495911]
50. Frei E, Spindler I, Grissmer S, Jager H. Interactions of N-terminal and C-terminal parts of the small conductance Ca^{2+} activated K^+ channel, hSK3. Cell Physiol Biochem. 2006; 18:165–176. [PubMed: 17167222]
51. Maylie J, Bond CT, Herson PS, Lee WS, Adelman JP. Small conductance Ca^{2+}-activated K^+ channels and calmodulin. J Physiol. 2004; 554:255–261. [PubMed: 14500775]
52. Zhang XD, Timofeyev V, Li N, Myers RE, Zhang DM, Singapuri A, Lau VC, Bond CT, Adelman J, Lieu DK, Chiamvimonvat N. Critical roles of a small conductance Ca^{2+}-activated K^+ channel (SK3) in the repolarization process of atrial myocytes. Cardiovasc Res. 2014; 101:317–325. [PubMed: 24282291]
53. Abdulkareem ZA, Gee JM, Cox CD, Wann KT. Knockdown of the small conductance Ca^{2+}-activated K^+ channels is potently cytotoxic in breast cancer cell lines. Br J Pharmacol. 2016; 173:177–190. [PubMed: 26454020]
54. Strobaek D, Hougaard C, Johansen TH, Sorensen US, Nielsen EO, Nielsen KS, Taylor RD, Pedarzani P, Christophersen P. Inhibitory gating modulation of small conductance Ca^{2+}-activated K^+ channels by the synthetic compound (*R*)-*N*-(benzimidazol-2-yl)-1,2,3,4-tetrahydro-1-naphtylamine (NS8593) reduces afterhyperpolarizing current in hippocampal CA1 neurons. Mol Pharmacol. 2006; 70:1771–1782. [PubMed: 16926279]
55. Carroll R, Gant VA, Yellon DM. Mitochondrial K_{ATP} channel opening protects a human atrial-derived cell line by a mechanism involving free radical generation. Cardiovasc Res. 2001; 51:691–700. [PubMed: 11530102]

56. Novalija E, Chen Q, Camara AK, Reiss M, Stowe DF. Anesthetic preconditioning triggered by reactive oxygen species also involves mitochondrial K_{ATP} channel opening in guinea pig isolated hearts. Anesth Analg. 2002; 94:S279.

57. Pain T, Yang XM, Critz SD, Yue Y, Nakano A, Liu GS, Heusch G, Cohen MV, Downey JM. Opening of mitochondrial K_{ATP} channels triggers the preconditioned state by generating free radicals. Circ Res. 2000; 87:460–466. [PubMed: 10988237]

58. Heinen A, Camara AK, Aldakkak M, Rhodes SS, Riess ML, Stowe DF. Mitochondrial Ca^{2+}-induced K^+ influx increases respiration and enhances ROS production while maintaining membrane potential. Am J Physiol Cell Physiol. 2007; 292:C148–C156. [PubMed: 16870831]

59. Holmuhamedov EL, Jovanovic S, Dzeja PP, Jovanovic A, Terzic A. Mitochondrial ATP-sensitive K^+ channels modulate cardiac mitochondrial function. Am J Phys. 1998; 275:H1567–H1576.

60. Akao M, O'Rourke B, Teshima Y, Seharaseyon J, Marban E. Mechanistically distinct steps in the mitochondrial death pathway triggered by oxidative stress in cardiac myocytes. Circ Res. 2003; 92:186–194. [PubMed: 12574146]

61. O'Rourke B. Pathophysiological and protective roles of mitochondrial ion channels, Review. J Physiol. 2000; 529:23–36. [PubMed: 11080248]

62. Di Lisa F, Bernardi P. Mitochondrial function as a determinant of recovery or death in cell response to injury. Mol Cell Biochem. 1998; 184:379–391. [PubMed: 9746332]

63. Ferrari R. The role of mitochondria in ischemic heart disease, Review. J Cardiovasc Pharmacol. 1996; 28(Suppl 1):S1–10. [PubMed: 8891865]

Abbreviations

APD	action potential duration
BSA	bovine serum albumin
CaMBD	Ca^{2+} calmodulin binding domain
COX	cytochrome *c* oxidase
CYPPA	*N*-cyclohexyl-*N*-[2-(3,5- dimethyl-pyrazol-1-yl)-6-methyl-4-pyrimidinamine
DCEB	5,6-dichloro-1-ethyl-1,3-dihydro-2H-benzimidazol-2-one
EDHF	endothelial hyperpolarizing factor
HR	hypoxia/reoxygenation
EBIO	1-ethyl-2-benzimidazolinone
EGFP	enhanced green fluorescent protein
IMM	inner mitochondrial membrane
IR	ischemia/reperfusion
LAD	left anterior descending coronary artery
mKHE	mitochondrial K^+/H^+ exchange
$\Delta\Psi_m$	mitochondrial membrane potential
mPTP	mitochondrial permeability transition pore

MCU	mitochondrial Ca^{2+} uniporter
MTR	mitotracker red
NS8593	*N*-[(1R)-1,2,3,4-tetrahydro-1-naphthalenyl]-1H-benzimidazol-2-amine hydrochloride
PPC	pharmacological pre-conditioning
RCI	respiratory control index
ROS	reactive oxygen species
RT-PCR	reverse transcription polymerase chain reaction
SK_{Ca}	small conductance Ca^{2+}-activated K^+ channel
TTC	2,3,5- triphenyltetrazolium chloride
TBAP	Mn(III) tetrakis (4-benzoic acid) porphyrin
TMRM	tetramethylrhodamine
TUNEL	terminal deoxynucleotidyl transferase (TdT)-mediated dUTP nick end-labeling
UCL 1684	6,10-diaza-3(1,3)8,(1,4)-dibenzena-1,5(1,4)-diquinolinacy clodecaphane

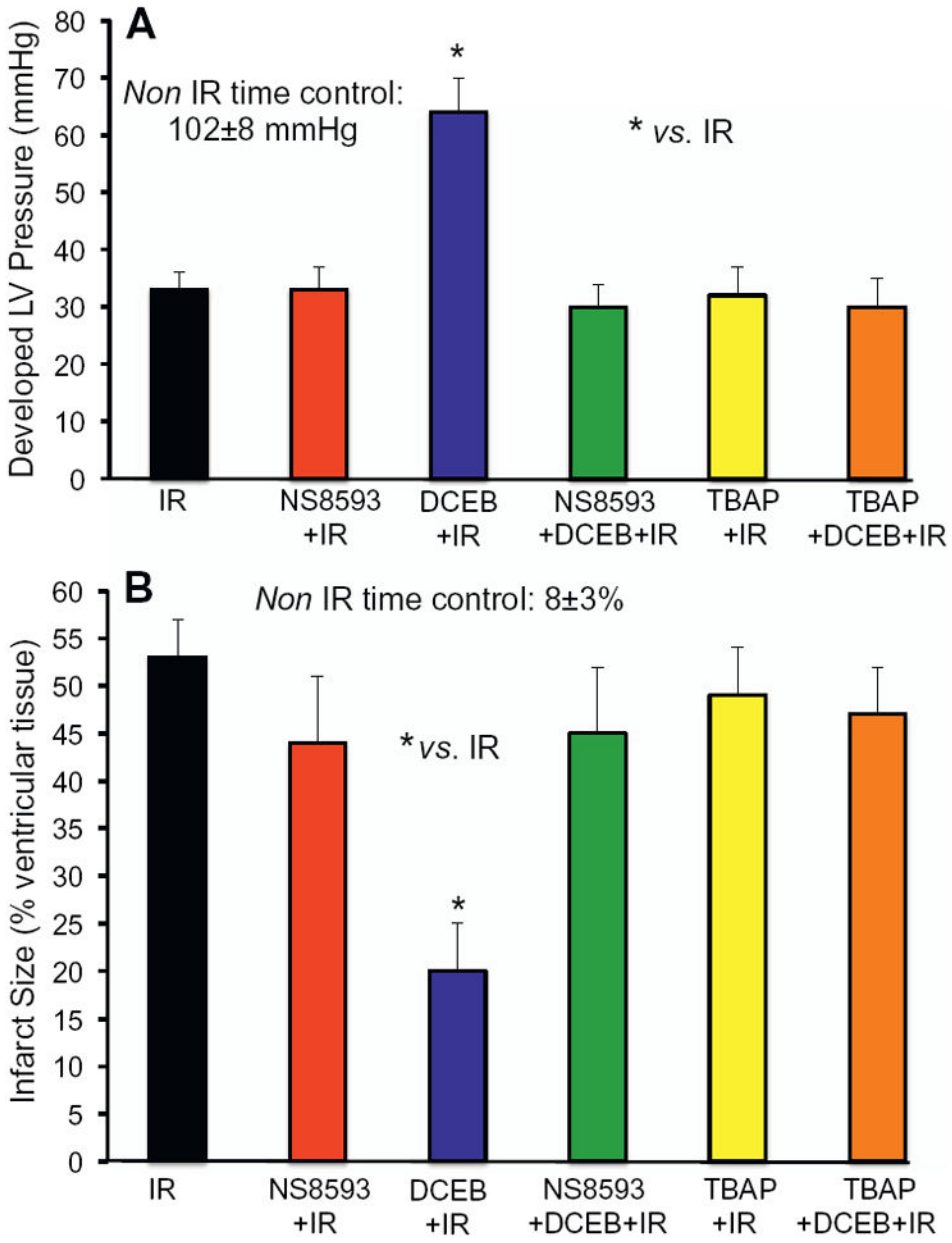

Fig. 1.

Developed (systolic-diastolic) LV pressure (A) and infarct size (B) after global IR injury in isolated guinea pig hearts perfused with vehicle (IR only), 3 μM DCEB (SK_{Ca} agonist) only, and with 10 μM NS8593 (SK_{Ca} blocker) or 5 μM TBAP (dismutator of $O_2\cdot$). Note that DCEB enhanced developed LVP (A) and reduced infarct size (B) *vs.* IR alone. NS8593 and TBAP had no effect when given alone but blocked protective effects of DCEB. $*P < 0.05$ *vs.* IR.

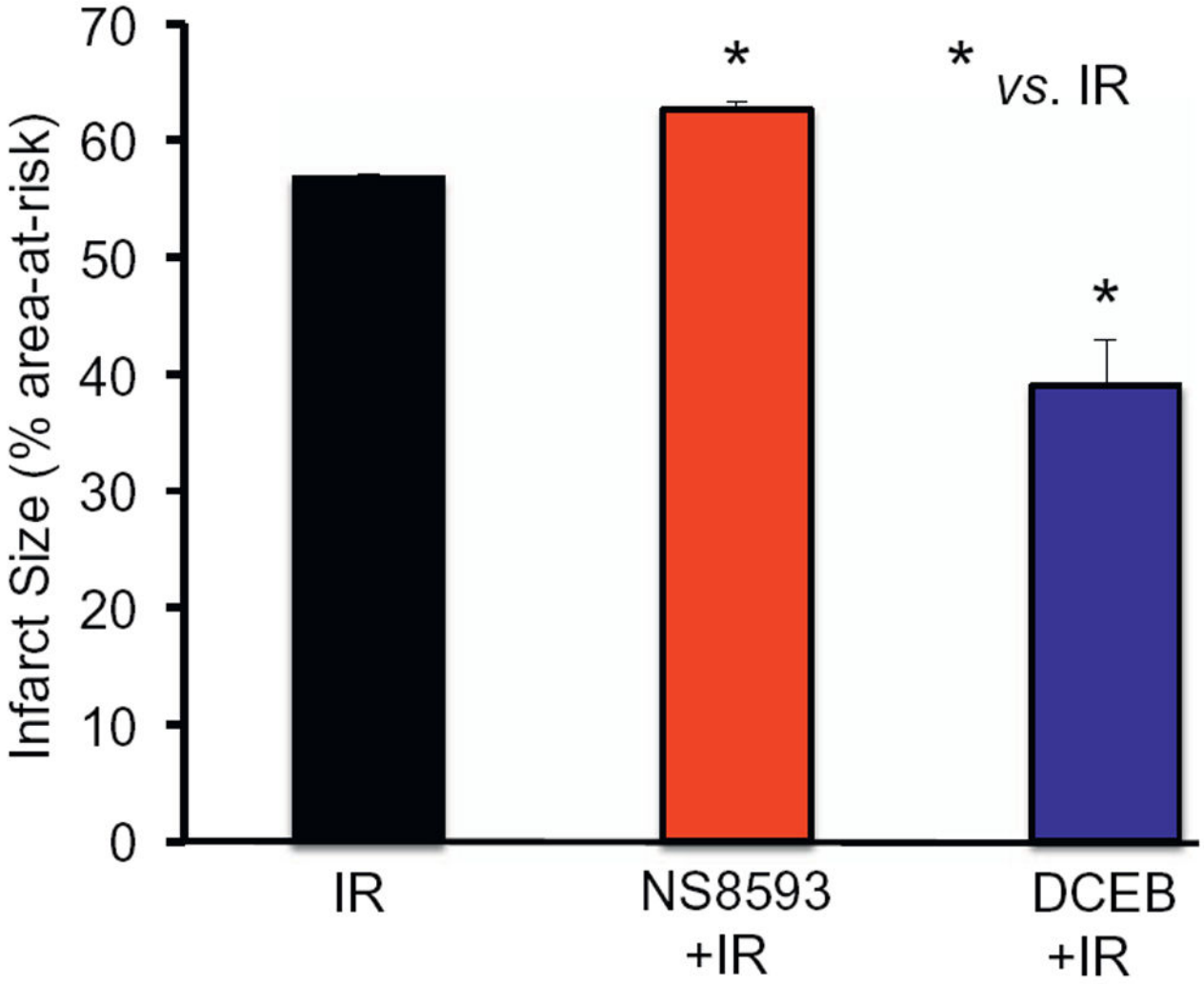

Fig. 2.

Infarct size (% area-at-risk) after regional ischemia (LAD occlusion) in intact rats infused i.v. with vehicle (IR only), NS8593, or DCEB. Note that *in vivo*, NS8593 infusion enhanced infarct size by about 10% *vs.* IR only, and that DCEB infusion reduced infarct size by about 42% *vs.* IR only. $*P < 0.05$ *vs.* IR.

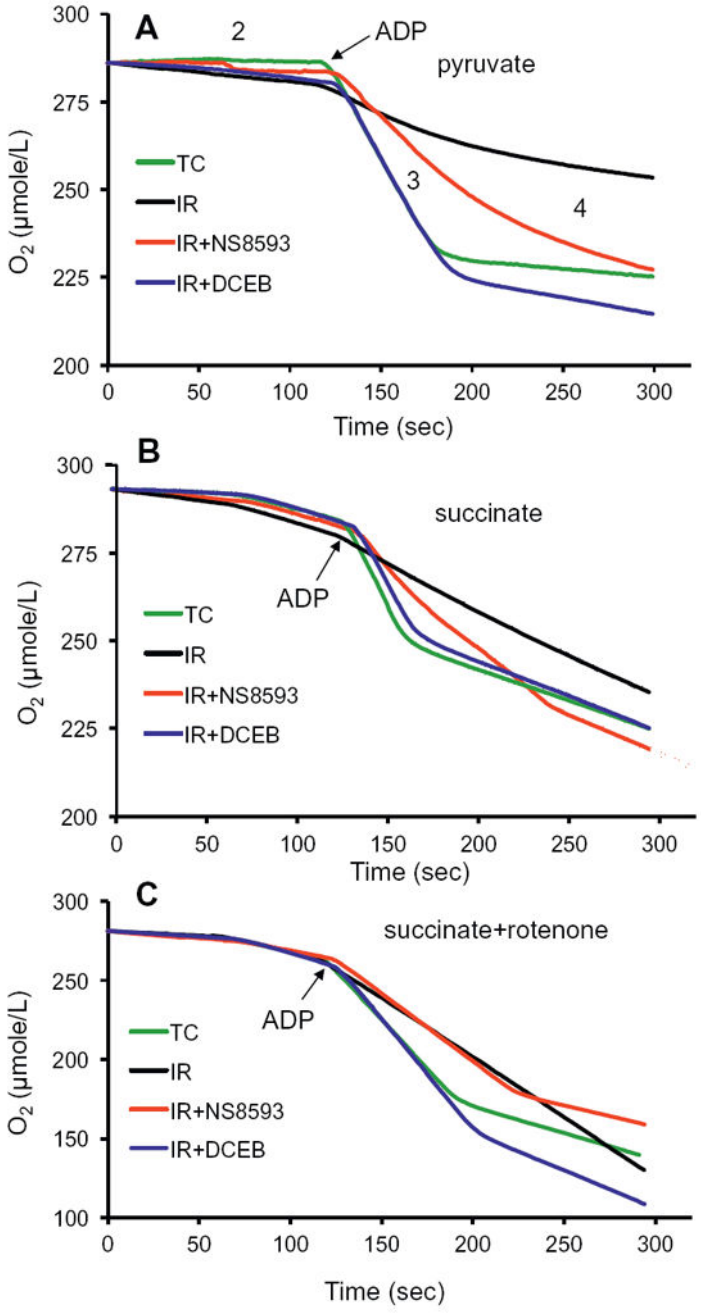

Fig. 3.

Comparative effects of SK_{Ca} channel agonist DCEB and SK_{Ca} antagonist NS8593 on O_2 consumption (respiration) in mitochondria isolated after 35 min global ischemia and 20 min reperfusion; TC: time controls. Traces represent typical respiration responses to complex I substrate (A), complex II substrate (B) and complex II substrate with rotenone (C). Note that RCI's were higher after hearts were treated with DCEB when compared to IR alone, and not significantly different after hearts were treated with NS8593 compared to IR alone. See Table 2 for complete respiration data and statistical significance.

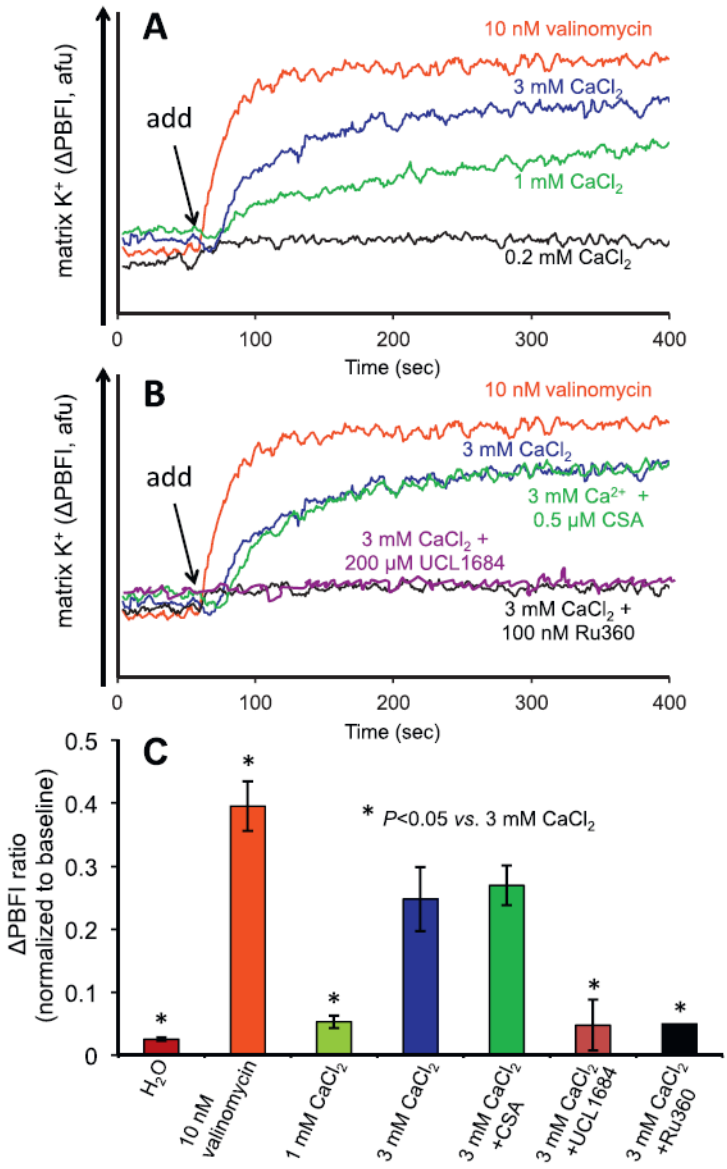

Fig. 4.

Representative changes in mitochondrial matrix K^+ levels (arbitrary fluorescence units, AFU) assessed using the K^+ binding fluorescent indicator PBFI-AM. A: K^+ influx induced by valinomycin (10 nM), different concentrations of $CaCl_2$. B: K^+ influx induced by 3 mM $CaCl_2$ without or with Ru360 (MCU inhibitor), UCL1684 (SK_{Ca} blocker) or cyclosporine A (CSA, an inhibitor of mPTP opening). C: Data summarized from 250 to 260 s with 2–3 measurements for each of two hearts. Note: Because of the presence of 2.5 mM EGTA, buffer and mitochondrial [Ca^{2+}] with added 0.2–3 mM $CaCl_2$ remain within the nM range.

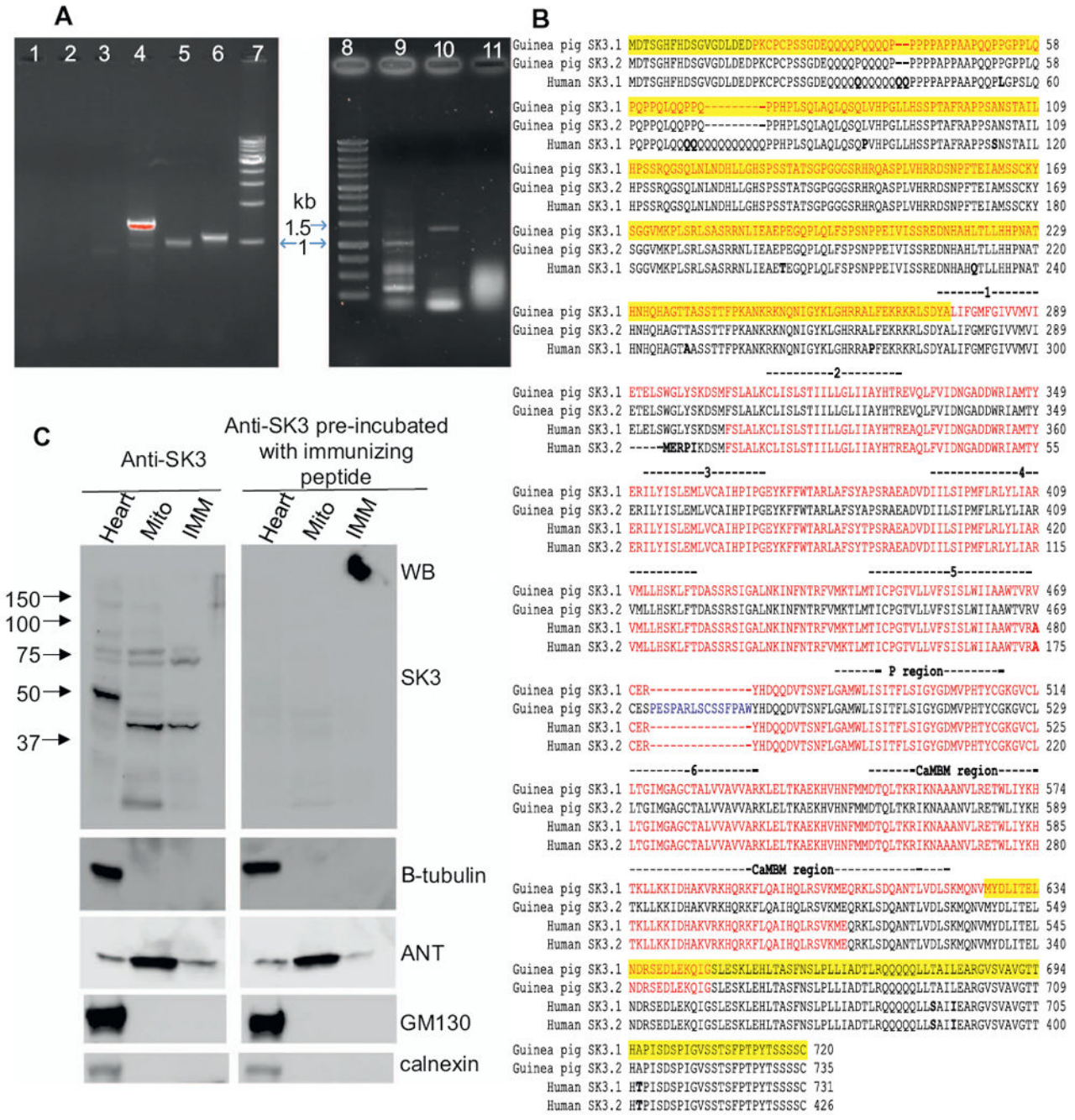

Fig. 5.

Expression of mSK_{Ca} channels in guinea pig hearts. A: A representative agarose gel analysis of RT-PCR amplified SK1, SK2 and SK3 from guinea pig cardiomyocytes (lanes 1–6) and human ventricular tissue (lanes 9–10). Lane 1: SK1-N; Lane 2: SK1-C; Lane 3: SK2-N; Lane 4: SK2-C; Lane 5: SK3-N; Lane 6: SK3-C; Lane 9: human SK3-N; Lane 10: human SK3-C; lanes 7 and 8: DNA ladder; Lane 11: RNA control. B: Alignment of SK3 splice variants. Red: deduced amino acid (a.a.) sequences from amplified genes; Blue: P-W sequence designating SK3.2; Black dashes: guinea SK3 transmembrane (T) domains 1–6;

CaMBD: Ca^{2+} calmodulin binding domain; Bold: human *vs.* guinea pig a.a. differences; Yellow: truncated N terminus (a.a. 1–277) or C-terminus (a.a. 627–720) of SK3.1 as overexpressed in HL-1 cells (Fig. 8). C: Western blot analyses of SK3 in guinea pig heart (Heart), heart mitochondria (Mito) and mitochondrial inner membrane (IMM). One membrane was incubated with specific primary antibody anti-SK3 (Alomone Lab APC-103) (SK3 left panel); another membrane was incubated with the same antibody, anti-SK3, but which was neutralized with the corresponding immunizing SK3 peptide before being added (SK3 preincubation, right panel). Tubulin, GM130, and calnexin were used to monitor purity of mitochondria and IMM; no contamination by cytosol, Golgi, or sarcoplasmic reticular membrane protein was observed in mitochondria and IMM. ANT was used to monitor integrity of mitochondria and IMM. Since SK3 expression is weak in mitochondria, the protein concentration loaded in the mito lane was larger than that in heart and IMM lanes.

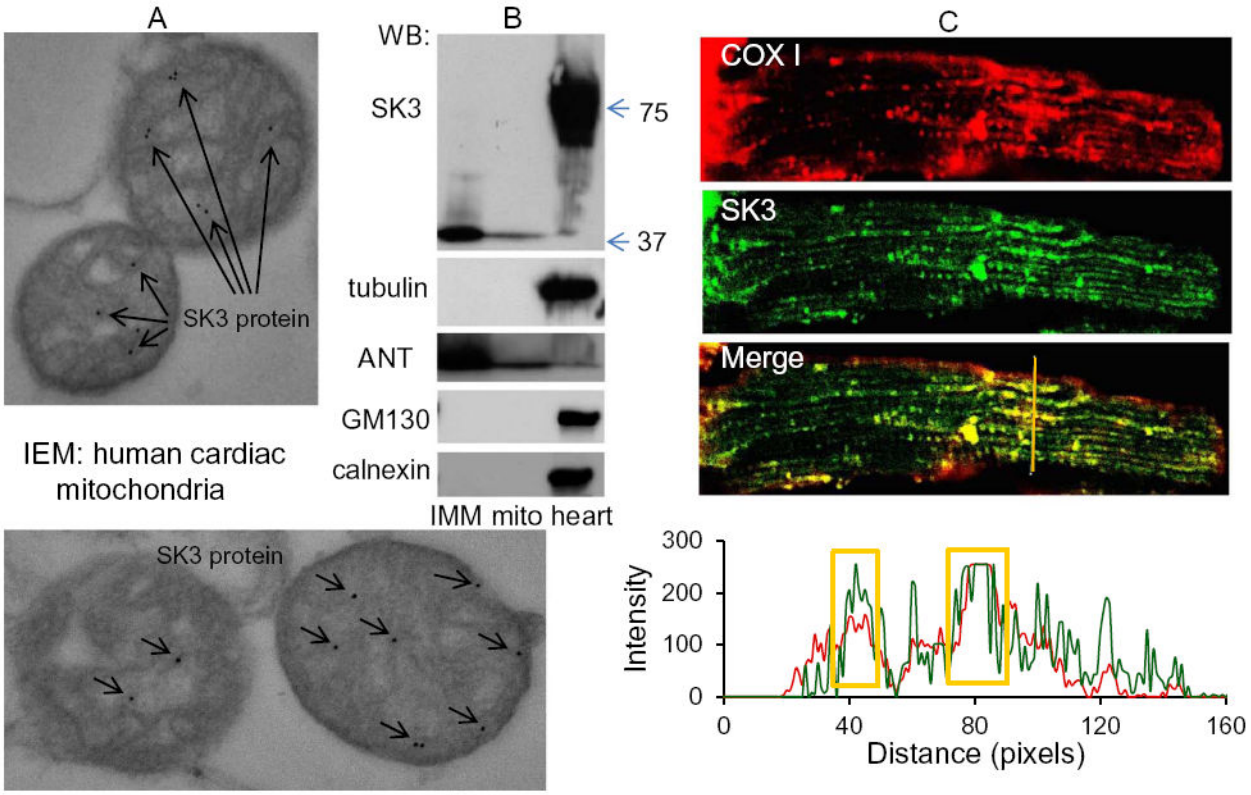

Fig. 6.

Location of mSK3 in human heart and rat cardiomyocytes. A: Immuno-electron microscopic (IEM) detection of isolated human ventricular mitochondria immunostained with specific antibody against SK3. B: Western blot analyses of SK3 expression in human ventricular tissue (heart), mitochondria (mito) and inner mitochondrial membrane (IMM). Tubulin confirmed purity of mitochondrial isolation, adenine nucleotide translocase (ANT) confirmed enrichment of mitochondria and IMM, and GM130 and calnexin confirmed absence of contamination by Golgi or sarcoplasmic reticulum membrane, respectively. C: Confocal fluorescence images of adult rat cardiomyocytes immuno-stained simultaneously with SK3 antibody followed by FITC conjugated secondary antibody (middle panel, Green) and COX 1 (cytochrome *c* oxidase) antibody, followed by Alexa Fluor 546 conjugated secondary antibody (top panel, red). Yellow color in merged image (bottom panel) depicts SK3 localized in mitochondria; the intensity profile panel showed the overlapping degree of SK3 with COX 1. The x-axis in the intensity profile is from top to bottom. The yellow rectangles label the overlap areas of SK3 with COX 1.

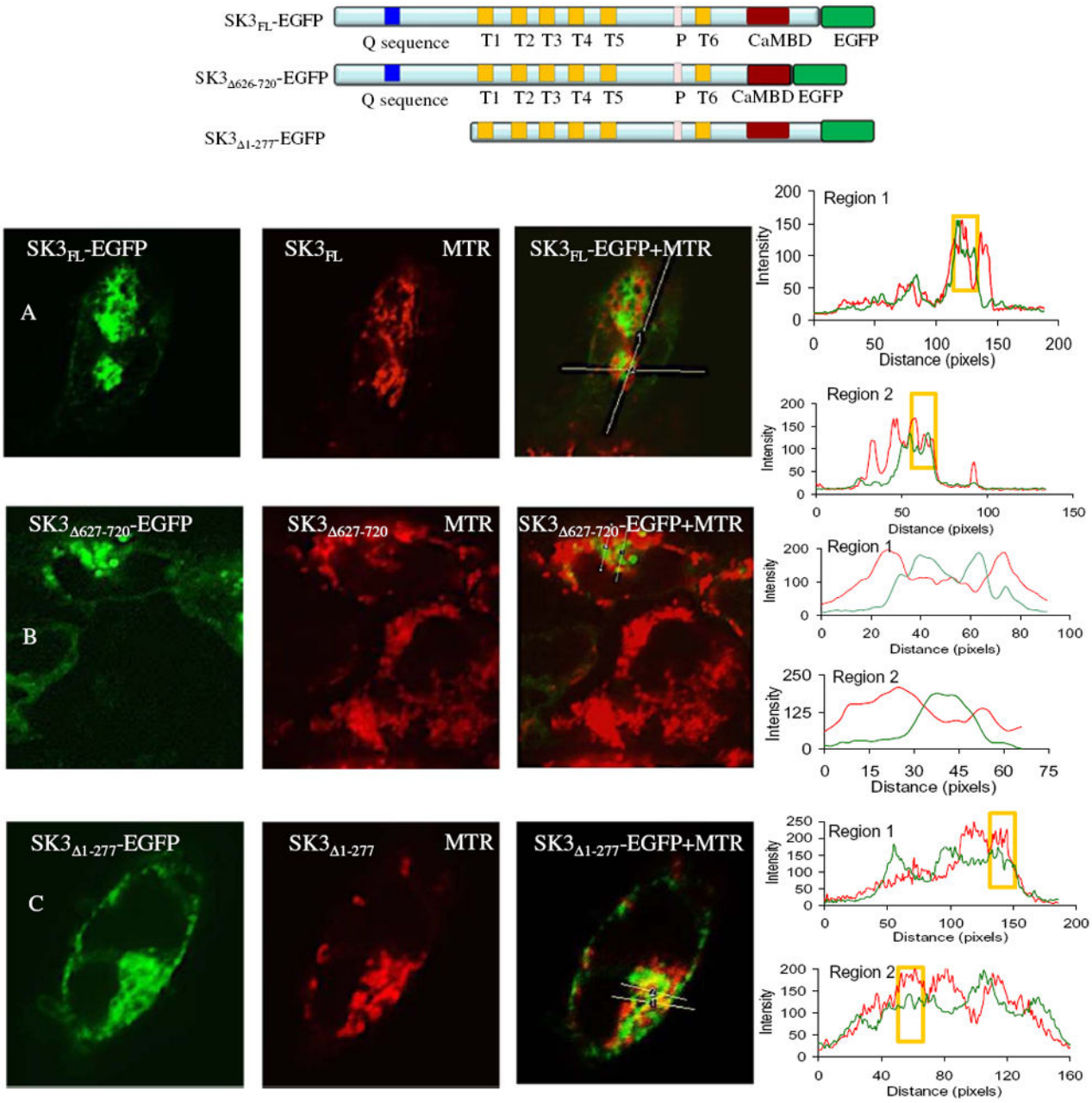

Fig. 7.

SK3.1 localized into mitochondria. Top panels: Schematic of $SK3_{FL}$-EGFP, $SK3_{\Delta1–277}$–EGFP and $SK3_{\Delta626–720}$–EGFP constructs. Q sequence, poly glycine sequence; T1–6, transmembrane regions; P, selectivity pore; CaMBD, Ca^{2+} calmodulin binding domain; EGFP, enhanced green fluorescence protein. Bottom panels: Confocal fluorescence images of HL-1 cells transfected with $SK3_{FL}$-EGFP (A, Green), $SK3_{\Delta626–720}$–EGFP (B, Green) or $SK3_{\Delta1–277}$–EGFP (C, Green) and stained with Mitotracker red, (MTR, Red). Merging (orange) depicts colocalization of SK3 with MTR; the intensity profiles show the overlapping degree of SK3 with MTR. The x-axis in the intensity profile was recorded from

top to bottom and from left to right for regions 1 and 2 respectively. The yellow rectangles label the overlap areas of SK3 with MTR.

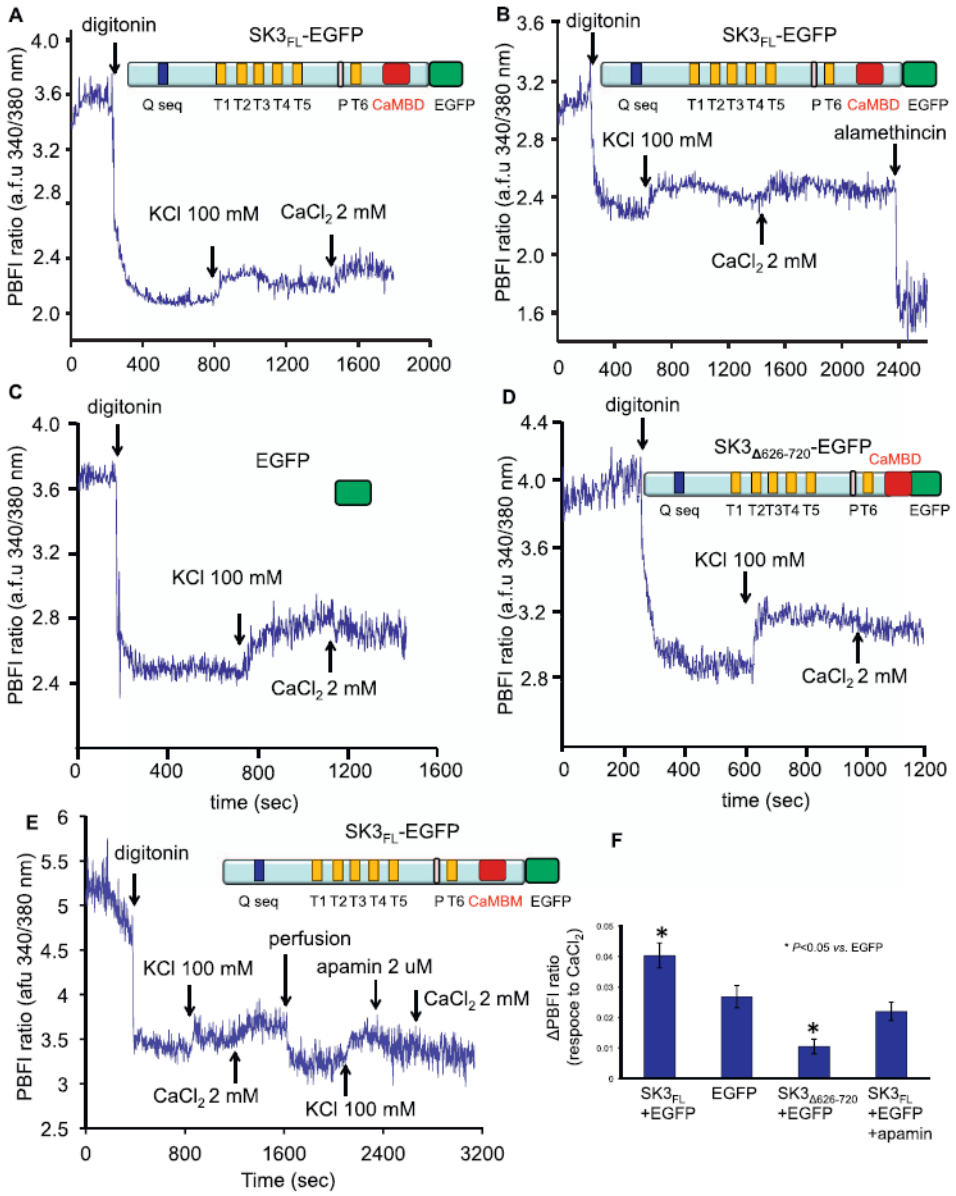

Fig. 8.

Representative recordings of mK^+ uptake activated by adding $CaCl_2$ to buffer in HL-1 cells transfected with SK3.1 constructs. Traces of PBFI fluorescence indicate changes in m $[K^+]$. A: in $SK3_{FL}$-EGFP transfected HL-1 cells; B: in $SK3_{FL}$-EGFP transfected HL-1 cells with alamethicin, a mitochondrial pore forming peptide; C: in pEGFP-N3 transfected HL-1 cells; D: in $SK3_{\Delta 626–720}$–EGFP transfected HL-1 cells; and E: in $SK3_{FL}$-EGFP transfected HL-1 cells with apamin, a blocker of the SK3 channel. F: averaged ΔPBFI ratios induced by adding $CaCl_2$ to permeabilized HL-1 cells. n= 20 cells; $*P < 0.05$ *vs.* EGFP control. Because of the presence of 3 mM EGTA and 5 mM $MgCl_2$, mitochondrial $[Ca^{2+}]$ with added 2 mM $CaCl_2$ remained within the nM range.

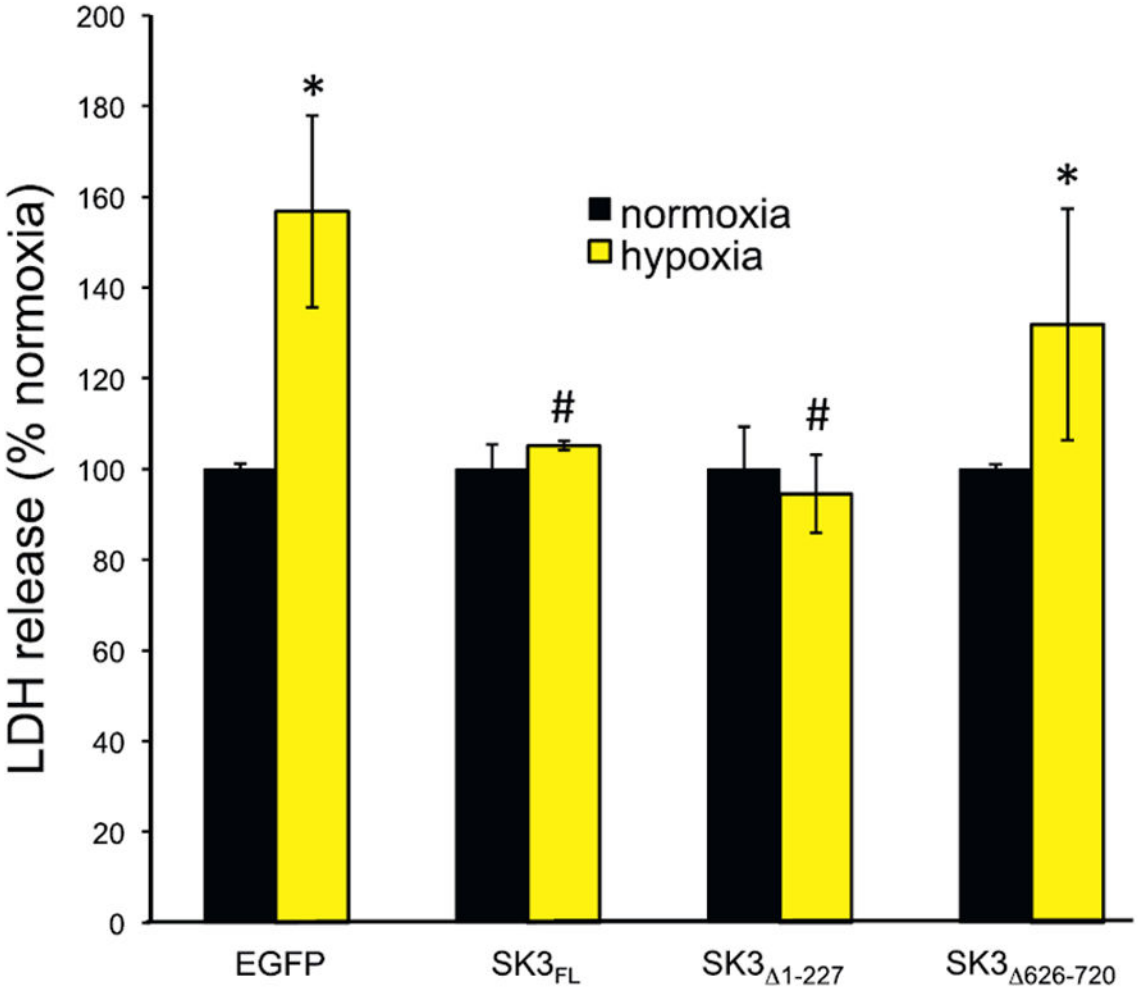

Fig. 9.

Lactate dehydrogenase (LDH) release is reduced if SK3 C-terminus is intact. HL-1 cells transfected with pEGFP-N3, $SK3_{FL}$, $SK3_{\Delta 1–277}$ and $SK3_{\Delta 626–720}$ were subjected to hypoxia/reoxygenation or normoxia. LDH activity was measured in the reoxygenation medium. Data presented are means ± SE from 3 independent experiments. $^{*}P < 0.05$ *vs.* normoxia groups, $^{\#}P < 0.05$ *vs.* EGFP groups.

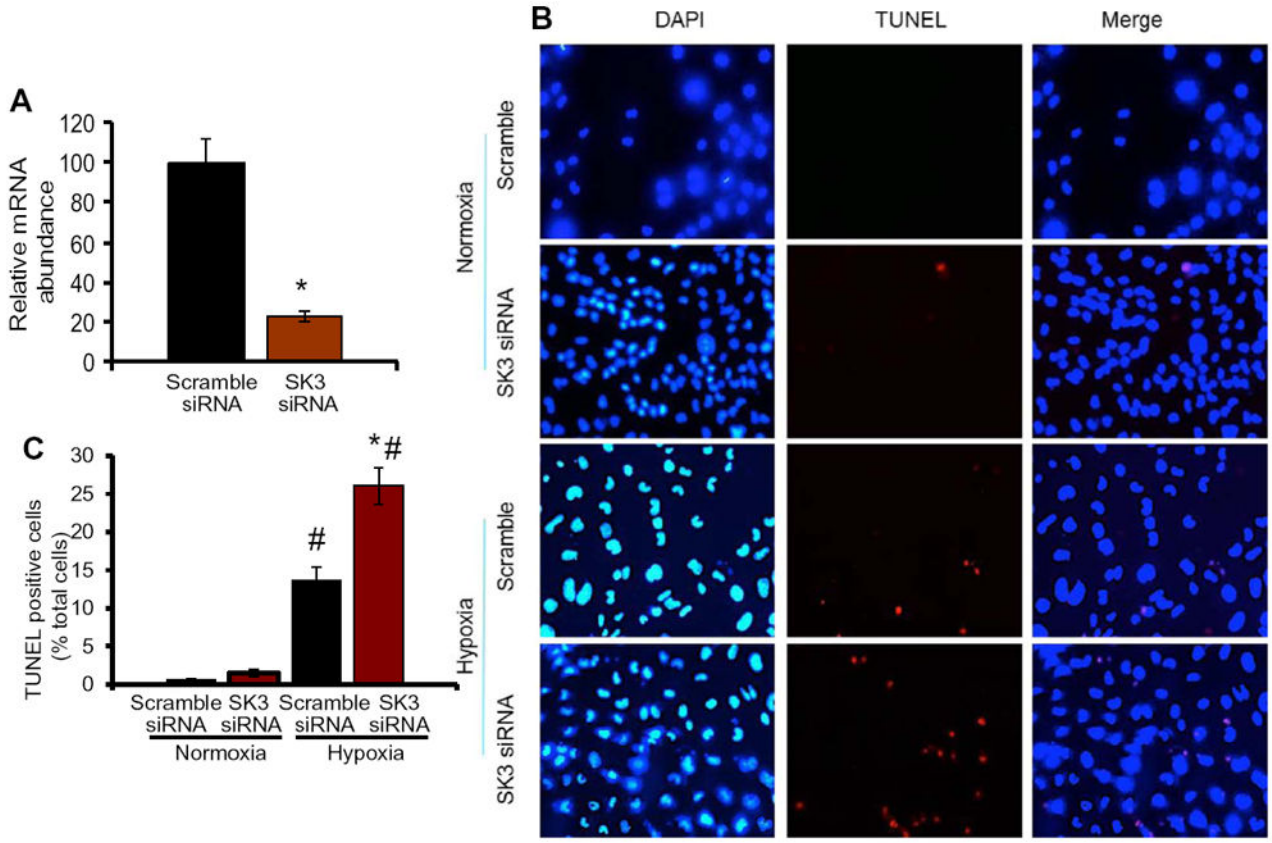

Fig. 10.

Silencing SK3 in HL-1 cells increases cell apoptosis. A: Real-time PCR assessment of SK3 relative mRNA abundance in HL-1 cells transfected with SK3 silence siRNA or scramble siRNA. Data presented are means ± SE from 3 independent experiments. * $P < 0.05$ *vs.* scramble siRNA groups. B: Representative TUNEL staining of HL-1 cells transfected with SK3 siRNA or scramble siRNA and subjected to normoxia (control) or to 2 h hypoxia and 16 h reoxygenation. Apoptotic nuclei were TUNEL stained (red) and counterstained with DAPI (blue) to label nuclei. C: Quantitative analysis of TUNEL-positive HL-1 cells. Mean ± SE, n = 2000 HL-1 cells per group. * $P < 0.05$ *vs.* scramble siRNA, $^{\#}$ $P < 0.05$ *vs.* normoxia.

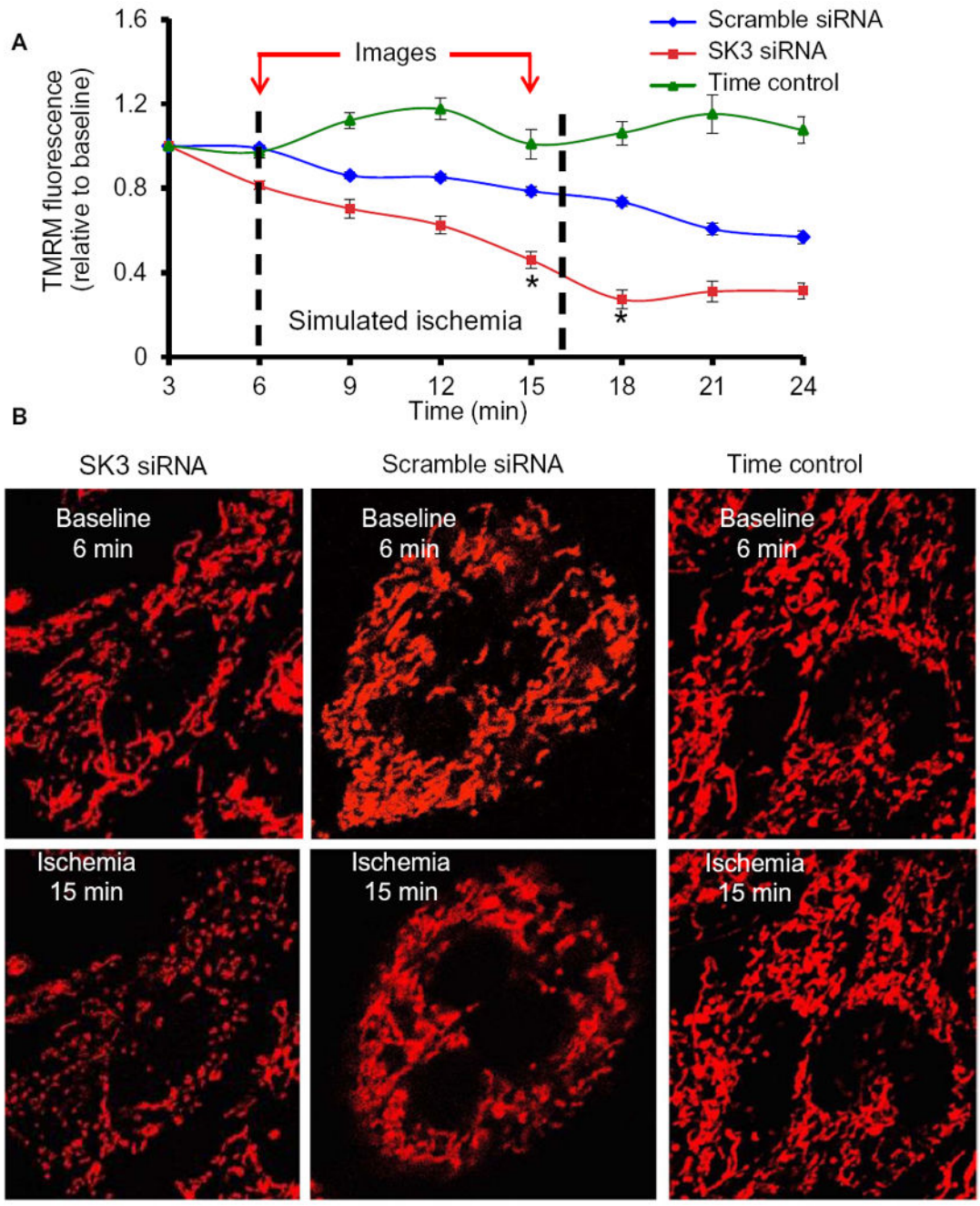

Fig. 11.

Silencing SK3 in HL-1 cells attenuates $\Delta\Psi_m$. HL-1 cells were transfected with SK3 silenced siRNA or scramble siRNA. Changes in TMRM fluorescence ($\Delta\Psi_m$) was measured in HL- 1 cells subjected to simulated ischemia (blocked respiration). A: Time course of relative changes in $\Delta\Psi_m$ was assessed in SK3 siRNA (n = 40 cells) or in scramble siRNA (n =50 cells) transfected HL-1 cells exposed to 10 min simulated ischemia followed by 8 min resuffusion of cells with normal Tyrode to wash out the simulated ischemia buffer and restore control conditions. (Time control = no ischemia; n =45 cells). $*P < 0.05$ *vs.* scramble

siRNA. B: Representative confocal images of TMRM fluorescence in HL-1 cells transfected with SK3 siRNA or scramble siRNA at conditions and times noted in A.

Table 1

Specific primers for three SKCa isoforms (SK1-3) amplification from mRNA of isolated guinea pig ventricular myocyte.

Name	GenBank #	Forward primer 5′- > 3′	Reverse primer 5′- > 3′	Range (bp)	Length (bp)
SK1-N	XM_003465180	ATGATCGGC CACAGCCGCAAT	GGTGATGGAGATAGCCACA	1–984	984
SK1-C	XM_003465180	AGCATCTCCTCCTGGGTCAT	CAGTCTGAGGGTCAGTGGC	871–1608	737
SK2-N	XM_003473180	ATGATCACTATACTCAGGTCCAGC	GGCACCGGA GGAGGC	1–999	999
SK2-C	XM_003473180	AGAAGAACCAGAACATCGGCTAC	AAG TTG GTG GCGCTGTAGAGG	1727–3109	1382
SK3-N	XM_003475583	ATGGACACT TCTGGGCACTT	AGCTGGACTTCGCGTGTATG	1–998	998
SK3-C	XM_003475583	CACCATCATCCTGCTGGGTT	CCTCCAGGATGGCAGTCAG	945-2050	1105

Biochim Biophys Acta. Author manuscript; available in PMC 2018 January 02.

Table 2

Respiration rates of isolated cardiac mitochondria energized with different mitochondria-targeted substrates after IR injury with or without SK_{Ca} agonist DCEB or antagonist NS8593.

	State 2	State 3	State 4	RCI
Pyruvate				
TC	6.7 ± 0.7	222.4 ± 23.5	11.4 ± 0.7	17.6 ± 2.6
IR	65.7 ± 0.7§	125.3 ± 53.2§	69.0 ± 27.0§	2.4 ± 1.1§
IR + NS8593	42.1 ± 3.4§	115.9 ± 44.3§	23.5 ± 12.1	5.0 ± 1.5§
IR + DCEB	6.0 ± 3.4*	179.6 ± 15.4	18.1 ± 4.7*§	10.2 ± 1.2*§
Succinate				
TC	65.0 ± 0.7	457.6 ± 38.6	79.7 ± 15.4	5.8 ± 0.4
IR	73.7 ± 9.4	203.7 ± 69.0§	114.6 ± 7.7§	1.9 ± 0.7§
IR + NS8593	58.3 ± 0.7	227.1 ± 69.0§	76.4 ± 16.8*	2.7 ± 0.4§
IR + DCEB	63.0 ± 8.1	345.1 ± 28.0*§	110.6 ± 8.7§	3.2 ± 0.2*§
Succinate + rotenone				
TC	63.0 ± 10.7	281.4 ± 57.0	77.1 ± 0.7	3.7 ± 0.5
IR	63.0 ± 5.4	113.2 ± 67.0§	100.5 ± 47.6	1.1 ± 0.6§
IR + NS8593	55.6 ± 4.7	117.3 ± 15.4§	85.1 ± 22.1	1.8 ± 1.0§
IR + DCEB	61.6 ± 14.7	255.3 ± 61.0*	102.5 ± 5.4§	2.6 ± 0.4*

Respiration rate (O_2 consumption, nmol/min/mg protein) was measured in cardiac mitochondria isolated at 20 min perfusion after 35 min global ischemia ± NS859 or DCEB given 20 min before and for 20 min after ischemia. RCI (respiratory control rate) = state 3/state 4. Time controls (TC) were not subject to ischemia but 75 min perfusion. n = hearts/group with 3–4 replicates within each mitochondrial pellet.

$^{*}P < 0.05$ *vs.* IR only.

$^{\S}P < 0.05$ *vs.* TC.